CYP enzymes, expressed within live human suspension cells, are superior to widely-used microsomal enzymes in identifying potent CYP1A1/CYP1B1 inhibitors: Identification of quinazolinones as CYP1A1/CYP1B1 inhibitors that efficiently reverse B[a]P toxicity and cisplatin resistance

Vinay R. Sonawane, Mohd Usman Mohd Siddique, Linda Gatchie, Ibidapo S. Williams, Sandip B. Bharate, Venkatesan Jayaprakash, Barij N. Sinha, Bhabatosh Chaudhuri

PII: S0928-0987(19)30069-7
DOI: https://doi.org/10.1016/j.ejps.2019.02.016
Reference: PHASCI 4846

To appear in: *European Journal of Pharmaceutical Sciences*

Received date: 20 September 2018
Revised date: 26 December 2018
Accepted date: 12 February 2019

Please cite this article as: V.R. Sonawane, M.U.M. Siddique, L. Gatchie, et al., CYP enzymes, expressed within live human suspension cells, are superior to widely-used microsomal enzymes in identifying potent CYP1A1/CYP1B1 inhibitors: Identification of quinazolinones as CYP1A1/CYP1B1 inhibitors that efficiently reverse B[a]P toxicity and cisplatin resistance, European Journal of Pharmaceutical Sciences, https://doi.org/10.1016/j.ejps.2019.02.016

CYP enzymes, expressed within live human suspension cells, are superior to widely-used microsomal enzymes in identifying potent CYP1A1/CYP1B1 inhibitors: Identification of quinazolinones as CYP1A1/CYP1B1 inhibitors that efficiently reverse B[*a*]P toxicity and cisplatin resistance

Vinay R. Sonawane[a,#], Mohd Usman Mohd Siddique[b,#], Linda Gatchie[a], Ibidapo S Williams[a], Sandip B. Bharate[c], Venkatesan Jayaprakash[b], Barij N. Sinha[b], Bhabatosh Chaudhuri[a,*]

[a] CYP Design Ltd, The Innovation Centre, 49 Oxford Street, Leicester, LE1 5XY, UK.

[b] Department of Pharmaceutical Sciences & Technology, Birla Institute of Technology, Mesra, Ranchi-835215, India

[b] Indian Institute of Integrative Medicine (CSIR), Canal Road, Jammu-180001, India.

[#] Contributed equally to the work described

* Corresponding author:

**Tel: 00-44-7805230121; E-mail: bchaud00@gmail.com (BC)*

ABSTRACT

Microsomal cytochrome P450 (CYP) enzymes, isolated from recombinant bacterial/insect/yeast cells, are extensively used for drug metabolism studies. However, they may not always portray how a developmental drug would behave in human cells with intact intracellular transport mechanisms. This study emphasizes the usefulness of human HEK293 kidney cells, grown in 'suspension' for expression of CYPs, in finding potent CYP1A1/CYP1B1 inhibitors, as possible anticancer agents. With live cell-based assays, quinazolinones **9i**/**9b** were found to be selective CYP1A1/CYP1B1 inhibitors with IC_{50} values of 30/21 nM, and >150-fold selectivity over CYP2/3 enzymes, whereas they were far less active using commercially-available CYP1A1/CYP1B1 microsomal enzymes (IC_{50}, >10/1.3-1.7 μM). Compound **9i** prevented CYP1A1-mediated benzo[a]pyrene-toxicity in normal fibroblasts whereas **9b** completely reversed cisplatin resistance in PC-3/prostate, COR-L23/lung, MIAPaCa-2/pancreatic and LS174T/colon cancer cells, underlining the human-cell-assays' potential. Our results indicate that the most potent CYP1A1/CYP1B1 inhibitors would not have been identified if one had relied merely on microsomal enzymes.

KEYWORDS: Microsomal CYP450 enzymes; cisplatin resistance; CYP1A1 inhibitors; CYP1A1-mediated benzo[a]pyrene toxicity; CYP1B1 inhibitors; hard to metabolize medications; live CYP-expressing human cells.

INTRODUCTION

Cytochrome P450 (CYP) enzymes belong to a superfamily of monooxygenase enzymes. The human CYP family consists of 57 proteins (Lewis, 2004). Around a dozen human CYP enzymes are responsible for the metabolism of xenobiotics, which include pharmaceutical drugs, chemicals and other substances that humans imbibe in their daily existence. These CYPs account for ~70-80% of liver enzymes involved in the metabolism of xenobiotics by the liver (Fasinu et al., 2012). In general, the liver CYPs enable conversion of hydrophobic molecules to water-soluble products, to facilitate excretion. Essentially, these CYPs bring about oxidation of chemicals, usually with the incorporation of polar moieties or removal of hydrophobic groups so as to render them soluble for excretion (Nebert et al., 2013).

At the pre-clinical stage of drug discovery, CYP enzymes play critical roles in the evaluation of metabolic profiles of drug-like candidates (Nebert and Russell, 2002). Human liver CYP enzymes are bound to human liver microsomes (HLMs) which are principally endoplasmic reticular (i.e. ER) membranes. Human CYPs bound to the ER of baker's yeast cells and insect cells or the periplasmic membranes of bacterial cells (since prokaryotic cells do not contain ER) are commonly used for pre-clinical drug development (Hausjell et al., 2018). Although microsomal CYPs isolated from such recombinant cells are accepted as in vitro tools for research linked to drug metabolism, they are not always able to predict how a compound would inhibit or be metabolized by a CYP enzyme within live human cells where intracellular compartments (and proteins contained in these compartments), responsible for transport of chemicals, are fully intact. Hence, a type of live liver cells (i.e. hepatocytes) are the most preferred in drug metabolism studies (Basu & Shaik, 2016). Unfortunately, hepatocytes are inherently inconsistent in their content because they are usually created from the pooling of a large number of livers derived from individuals who do not share similar

genetic makeup. Hepatocytes provide reproducible results only after extensive initial standardization. Therefore, an alternative technology that would eliminate the negative aspects of hepatocytes and isolated microsomal enzymes but would preserve their positive features could be useful in facilitating drug discovery research.

This report compares, for the first time, screening of a small chemical library with the help of (a) CYP-expressing live human kidney (HEK293) cells, grown in 'suspension' (it should be noted that hepatocytes are also grown in 'suspension'), and (b) microsomal CYP enzymes, in the identification of inhibitors of CYP1A1 and CYP1B1, two CYP enzymes which have critical roles in the genesis of cancer. Unlike microsomal enzymes and hepatocytes which lose all CYP activity within a few hours (i.e. a maximum of 6 h) at 37 ºC (Donato et al., 2004), we see that CYP activities within live whole cells can be maintained over 4-5 days. CYP activities, expressed within live HEK293 'suspension' (HEK293S) cells, also do not suffer from the drawback of being inherently dependent on a NADPH-regenerating system, which is absolutely essential for all microsomal assays (Mazur et al., 2009). Our results from screening of this chemical library indicate that there are stark differences in the inhibition of cellular CYP1A1 and CYP1B1 enzymes when compared with the inhibition of the same enzymes isolated as microsomal entities from baker's yeast (Sacchrosomes™; CYP Design Ltd), from insect cells (Supersomes™; Corning) or from bacteria (Bactosomes™; Cypex). The company Invitrogen (Thermo-Fisher) also markets CYP-microsomes (Baculosomes™) isolated from insect cells; however, they do not sell the human CYP1A1 and CYP1B1 microsomal enzymes.

The CYP1A1 enzyme, belonging to the CYP1 sub-family, mediates the metabolism of polyaromatic hydrocarbons (PAHs) (Moorthy et al., 2015). PAHs, such as benzo[a]pyrene (B[*a*]P) and 7,12-dimethylbenz(a)anthracene (DMBA), are present in cigarette smoke and

charcoal-broiled foods. PAHs form diol-epoxides and *o*-quinones which intercalate DNA at the DNA synthesis (S) phase of the cell division cycle, and thereby cause mutations in DNA which lead to carcinogenesis. It has been reported that this is one of the main causes of lung cancer. Hence, it has been inferred that inhibition of CYP1A1 enzyme can prevent lung cancer (Moorthy et al., 2015; Androutsopoulos et al., 2009). It has also recently been published that hyperactive CYP1A1 effects intestinal homeostasis in mice which leads to colon cancer (Schiering et al., 2017).

The CYP1B1 isoform, also of the CYP1 sub-family, mainly mediates hydroxylation of endobiotics, chemicals endogenous to the human body, such as estradiol and fatty acids. CYP1B1 is unusual amongst CYP proteins. It is the only CYP which is not present in normal healthy tissues but is significantly overexpressed in most hormonal cancers that are linked to the ovary, prostate, uterus, mammary glands, pituitary. Overexpression of CYP1B1 is unrelated to the genetic origin of these cancers (McFadyen et al., 1999; Murray et al., 1997; Muskhelishvili et al., 2001; Gajjar et al., 2012; Sutter et al., 1994; Carnell et al., 2004). It has been shown that in cancer and precancer tissues of the mammary, prostate and ovary, CYP1B1 mediates regio-specific conversion of estradiol to 4-hydroxy estradiol (4-OHE2) while CYP1A1 catalyzes the formation of 2-hydroxy estradiol (2-OHE2). Only the 4-OHE2 metabolite, not 2-OHE2, induces oncogenesis (Yager, 2000). In cancer cells, 4-OHE2 is further oxidized to 2,3-estradiol quinone and 3,4-estradiol quinone, which are initiators of tumor formation. 2,3-Estradiol quinone forms a stable adduct with DNA, whereas binding of 3,4-estradiol quinone to DNA results in its depurination that leads to genotoxic mutations (Cavalieri et al., 2002; Cavalieri et al., 1997; Hayes et al., 1996; Rogan et al., 2003; Zhu & Conney, 1998; Rochat et al., 2001; Newbold & Liehr, 2000; Cavalieri & Rogan, 2004; Liehr & Ricci, 1996). Overexpression of CYP1B1 in the endometrium, mammary and ovarian tissues is now considered as a biomarker for hormonal oncogenesis (Liehr & Ricci, 1996;

Spink et al., 1998; Tait et al., 1990). CYP1B1 overexpression also leads to the inactivation of (i.e. resistance to) various cancer drugs such as *trans*-tamoxifen (Crewe et al., 2002), docetaxel (Chang et al., 2015), cisplatin and nucleoside analogues (Martinez et al., 2008) in diverse cancer cell types. Hence, it has been proposed that CYP1B1-specifc inhibitors should be able to reverse resistance to such widely used anticancer agents.

In previous studies (Horley et al., 2017; Mohd Siddique et al., 2016; Mohd Siddique et al., 2017; Joshi et al., 2017), we have successfully identified new structural classes of potent CYP1A1 and CYP1B1 inhibitors using Sacchrosomes™ and live human HEK293 cells. However, we have never attempted a rigorous head-to-head comparison of the results obtained from the two dissimilar assay systems although there have been hints that there may be some differences between a compound's ability to inhibit CYP1A1/CYP1B1 in Sacchrosomes-based microsomal assays and live human cells. Here, we show clearly that the sole use of microsomal CYP enzymes, Sacchrosomes™, Supersomes™ and/or Bactosomes™ would not have identified molecules that are potent CYP1A1 and CYP1B1 inhibitors. Instead, live 'suspension' human kidney cells, which express CYP enzymes intracellularly, were essential for the revelation of compounds with possible therapeutic potential.

We have earlier reported biphenyl urea and quinazolinone derivatives as highly selective and potent CYP1B1 inhibitors (Mohd Siddique et al., 2016; Mohd Siddique et al., 2017). In continuation of these efforts, we have now further explored the quinazoline scaffold to discover potent inhibitors of both CYP1A1 and CYP1B1, using the live human cell system, in parallel with the use of microsomal enzymes. We show that presence of bulkier side-chains on *meta* and *para*-positions of the aryl ring at position 2 of quinazolinones establish favorable H-bonding and hydrophobic interactions with amino acid residues within the active sites of these enzymes, while keeping the quinazolinone ring close to heme. An additional –NH-CO-

group, incorporated in the side-chain, improves polar interactions that may, in turn, improve the potency of this class of drugs. Furthermore, we have profiled the CYP1A1 and CYP1B1 inhibitors, identified in the human cell system, as true inhibitors of the two enzymes. The CYP1A1 inhibitors rescue CYP1A1-overexpressing normal fibroblast cells from B[*a*]P-mediated toxicity while the CYP1B1 inhibitors overcome cisplatin resistance in multiple cancer cells that overproduce CYP1B1.

RESULTS AND DISCUSSION

Development of CYP-expressing HEK293 Cellular Assays for Screening of CYP Inhibitors and Drug Metabolism Studies

Adaptation of HEK293 Monolayer Adherent Cells for Growth as 'Suspension' Cultures. In the early stages of drug discovery, recombinant proteins expressed transiently in mammalian cells are considered to be an important alternative to stable gene expression since chromosomal integration of DNA is time-consuming and costly (Daramola et al., 2013; Meissner et al., 2001). Transient expression of recombinant proteins in several mammalian cell lines has been demonstrated successfully (Flied et al., 2015; Han et al., 2007). In this study, attempts have been made to express major CYP enzymes transiently in human kidney HEK293 cells, grown in 'suspension' (i.e. HEK293S cells), so that metabolically-active, whole live cells could be used to demonstrate their application in screening of chemical libraries.

Until recently, CYP assays have never been performed in live recombinant human 'suspension' cells that overexpress specific human CYP enzymes of interest. In the past, CYP enzyme expression has been attempted in adherent cell cultures. Upon harvesting the cultures, the metabolically-inactive cells yielded quite poor activity with fluorogenic

substrates (Donato et al., 2004). We have now adapted 'adherent' HEK293 cells (Figure 1A) for growth in 'suspension'. The cells in 'suspension' have been re-named as HEK293S cells (Figure 1B). Around 30% transfection efficiency (Figures 1C to 1E) was seen when HEK293S cells were co-transfected with two separate plasmids, one encoding the human CYP1A1 gene and the other encoding the gene for the enhanced green fluorescent protein (eGFP).

Establishment of the Live HEK293S Cell CYP-expression System for Screening of CYP Inhibitors. HEK293S cells, suspended in 100 mL culture medium in polycarbonate shake flasks, were transfected with expression plasmids containing either the human CYP1A1 or the human CYP1B1 genes (Supplementary Information, SI; Figure S1 and S2). The expression of CYP1A1 and CYP1B1 proteins, in HEK293S cells, was confirmed by Western blotting (Figures 2A and 3A, respectively). The activities of the CYP1A1 and CYP1B1 enzymes were assessed (Figures 2B and 3B, respectively). The kinetics of CYP1A1 and CYP1B1-mediated reactions, with the fluorogenic compound 7-ethoxyresorufin (7-ER) as substrate, were found to be linear until 7-ER became limiting. The activities of CYP1A1 and CYP1B1 enzymes, in live cells, were monitored up to 120 h post-transfection (Figures 2C and 3C, respectively). It should be noted that CYP enzyme activity in microsomal enzyme assays and in hepatocytes become immeasurably small within 6 h of incubation at 37 ºC (Basu & Shaik, 2016; Donato et al., 2004). Reliability of CYP1A1/CYP1B1 enzyme activities, produced within recombinant HEK293S cells, was corroborated by testing for their inhibition by the FDA-recommended CYP1A1/CYP1B1 inhibitor, α-naphthoflavone (ANF; Figures 2D and 3D, respectively).

The CYP enzymes, 1A2, 2C9, 2C19, 2D6 and 3A4, which metabolize >80% of approved pharmaceutical drugs, were expressed similarly to CYP1A1/CYP1B1, in HEK293S cells.

The expression of the individual proteins from different plasmids (Supporting Information, Figures S3 to S7), the kinetics of their enzyme activities, their activities over 120 h of culture and their ability to be inhibited by FDA-recommended inhibitors were also studied (Supporting Information, Figures S8 to S12; and Table 1).

The IC_{50} values obtained in live HEK293S cells (Table 1), grown in 'suspension', were found to be in good agreement with the data reported in the literature for hepatocytes which normally are also grown in 'suspension'. This would indicate that the active site 3D geometry of recombinant enzymes within live HEK293S cells and hepatocytes are similar. However, our IC_{50} data obtained in HEK293S cells and that published in hepatocytes have some obvious inconsistencies with the data that have been described in the literature for human liver microsomes (HLMs) and recombinant microsomes (see Table 1).

Screening for CYP1 Inhibitors in a Chemical Library of Quinazolinones using CYP1-expressing HEK293 Cells and Microsomal Enzymes, followed by SAR Studies

Chemistry. Previously, we had described (Mohd Siddique et al., 2017) a simple and efficient route to constructing quinazoline-4-(*3H*)-ones (depicted in Scheme 1) via condensation of 2-amino benzamide with an aldehyde using DMF as a solvent. Sodium acetate was used as a base while *in situ* oxidation was performed by iodine. The rare substituted aldehydes were prepared separately, as depicted in Scheme 1. Various substituted anilines were treated with chloroacetyl chloride to prepare acetamide **1**. The reaction was carried out in glacial acetic acid at room temperature. The resultant acetamide was then reacted with 4-hydroxy benzaldehyde (**2a**), vanillin (**2b**) or isovanillin (**2c**) in presence of potassium carbonate and potassium iodide using acetone as solvent under reflux conditions. The prepared aldehydes **3, 6 & 8** were condensed with 2-amino benzamide (**4**) in DMF at 60-

70 °C, to synthesize the quinazolinones **5a-i, 7a-g**, **9a-k**. The compounds were purified simply via washing with ethyl acetate and petroleum ether in 40:60 ratio.

Screening for CYP1B1 and CYP1A1 Inhibition in Sacchrosomes™, Bactosomes™, Supersomes™ and Live HEK293S Cells Expressing CYP1A1 or CYP1B1 Enzymes. At first, all the 27 quinazolinones in the chemical library, that had been synthesized, were evaluated for inhibition of CYP1A1 and CYP1B1 only in microsomal enzyme assays using (i) Sacchrosomes™ (ER membrane-bound CYP1A1 or CYP1B1 enzyme, isolated from recombinant baker's yeast cells), (ii) Supersomes™ (ER membrane-bound CYP1A1 or CYP1B1 enzyme isolated from recombinant insect cells), and (iii) Bactosomes™ (periplasmic membrane-bound CYP1A1 or CYP1B1 enzyme isolated from recombinant bacterial cells). Later, live human HEK293 'suspension' cells (i.e. HEK293S cells), which contained plasmids bearing the human CYP1A1 gene or the human CYP1B1 gene, were used for assessing enzyme inhibition by the compounds.

The results obtained from microsomal and live HEK293S-cell-based assays are shown in Tables 2-4. Some of the compounds displayed IC_{50} values at low nanomolar concentrations, in live HEK293S cells. Surprisingly, these IC_{50} values were at variance to the values obtained in the microsomal assays using Sacchrosomes™, Supersomes™ and Bactosomes™. Moreover, compounds which had minimal activity at 10 µM concentrations in the initial microsomal assays were found to be quite active in the inhibition of CYP1A1 or CYP1B1 enzymes expressed within live HEK293S cells.

For example, compound **9i** showed no measurable CYP1A1 or CYP1B1 inhibitory capacity, at 10 µM concentration, in microsomal enzyme assays whereas it inhibited the CYP1A1 enzyme, expressed within HEK293S cells, with an IC_{50} of 30 nM (Table 4). Compound **9i** was the most potent CYP1A1 inhibitor that was identified in HEK293S cells

and it had >250-fold specificity with respect to CYP1B1, where the IC_{50} for inhibition was 7.8 μM in HEK293S cells (Table 4). Similarly, compound **7g** was identified as a potent CYP1A1 inhibitor only in HEK293S cells (IC_{50}, 60 nM; Table 3); in CYP1A1 microsomal assays, IC_{50} values ranged from 4.7 to 5.7 μM. Compound **7g** was also specific to CYPA1 vis-à-vis CYP1B1 (>75-fold specificity); the CYP1B1 IC_{50} value in HEK293S cells was 4.6 μM (6.5-7.8 μM in microsomal assays; Table 3).

Parallel experiments with CYP1B1 enzyme showed that compound **9b** had the best potency in inhibiting CYP1B1 expressed within HEK293S cells; the IC_{50} value was only 21 nM which was much lower than the IC_{50} values of 1.3-1.7 μM obtained using isolated CYP1B1-bound microsomes (Sacchrosomes™, Bactosomes™ and Supersomes™; Table 4). Likewise, compound **5e** inhibited CYP1B1 enzyme, expressed within live HEK293S cells, with an IC_{50} value of 42 nM whereas, using CYP1B1 microsomal enzymes, the IC_{50} values ranged from 4.1 to 5.1 μM (Table 2). However, compound **5e** was found to be similar in its inhibition of CYP1A1 and CYP1B1 in microsomal assays (CYP1A1/CYP1B1 IC_{50} values ranged from 4.1 to 6.9 μM). Both compounds **5e** and **9b** were specific (i.e. >100-fold specificity) to CYP1B1 when their IC_{50} values were compared with inhibition of CYP1A1. CYP1A1 IC_{50} value, in HEK293S cells, was >20 μM (compared to 6.1-6.9 μM in microsomes) for compound **5e**, and 2.3 μM (compared to >20 μM in microsomes) for compound **9b** (Tables 2 and 4).

It was also noticed that there was no clear difference in CYP1B1 inhibition by compound **7c** when tested in HEK293S cells and in microsomes (Table 3). In contrast, compound **7b** (having the -OMe group in position 2 rather than in position 3 of the aromatic ring 'C' as in **7c**) was specific to CYP1B1 (IC_{50}, 32 nM, with >180-fold specificity with respect to inhibition of CYP1A1 in the HE293S-cell-assays).

In summary, there appears to be a close correlation between enzyme inhibition in microsomal assays and within live cells in the synthesized quinazolinones **5a** to **5d**, **5f**, **5i**, **7a**, **7c** to **7f**, **9d** to **9h**, **9j** and **9k** (a total of 18 compounds). However, there was a clear difference in the inhibition of CYP1A1 and CYP1B1 enzymes, within HEK293S cells and those that are bound to microsomal membranes, by the rest of the 9 compounds in the quinazolinone library. Comparison of the results obtained in the HEK293S-cell-assays and the microsomal enzyme assays (in Tables 2-4) undoubtedly suggest that one would have missed the potent inhibitors of CYP1A1/CYP1B1 enzymes if one had relied merely on the initial screening of compounds with the microsomal CYP1A1/CYP1B1 enzymes.

The discrepancy between IC_{50} values determined using whole HEK293 cells and microsomes for some of the compounds in the chemical library may not be because of problems of outer cell wall permeabilization. We obtain very low IC_{50} values with CYP-expressing whole cells compared to the values obtained with enzymes bound to endoplasmic reticular (ER) (i.e. microsomal) membranes, the ER membranes being far more permeable than the outer cell wall. We think that, in whole cells, the specific proteins existing in the ER, and perhaps the vesicular proteins in the ER to Golgi secretory pathway (i.e. ER to Golgi transporters) may have a role to play on enzyme activity of CYPs bound to microsomal membranes. In the presence of tunicamycin (that inhibits glycosylation of ER proteins) and brefeldin (which blocks ER to Golgi traffic), IC_{50} values of the compounds that are low using CYP-expressing HEK293 cells increase perceptibly, resembling those obtained with microsomal enzymes (unpublished observations). That is why we think that the CYP-expressing HEK293 cells are more akin to hepatocytes rather than human liver microsomes (HLMs) which only contain ER proteins but are devoid of Golgi membrane proteins and also vesicular proteins (unpublished observations).

The observations with recombinant HEK293S cells would indicate that there exists a key SAR feature of the quinazolinones for inhibition of CYP1A1 and CYP1B1. As substitution at R1 position in all the three series are different, the structure-activity relationship write-up considered only the compounds with similar substitutions among the three series. In compound series **5a-i** having oxy-acetamide substitution at 4th position of ring C, Compounds **5g** & **5h** having naphthyl substitution and compounds **5d** & **5e** having phenyl ring with electron-withdrawing substitutions were found to be active and selective towards CYP1B1 (Table 2). Introduction of methoxy group *ortho* to oxy-acetamide group on ring C, reverses the selectivity and increase the potency of compound **7g**, in comparison with **5g** (Table 3 & 2). Compounds having electron-donating (**7b**-**7e**) as well as electron-withdrawing (**7f**) groups are now active and the one having *ortho*-methoxy (**7b**) exhibited potent and selective inhibition of CYP1B1 with IC_{50} of 0.032 μM (Table 3). Reversing the position of oxy-acetamide and methoxy groups provided **9a-k** series. This series of compounds provided the most potent and selective inhibitor of both CYP1A1 and 1B1 isoforms. Compound **9b** with *ortho*-methoxy substitution displayed improved potency in comparison with **7b**, while **9i** with *para*-fluro exhibited reversal of selectivity with improved potency in comparison with **7f** (Table 4 & 3). In summary, oxy-acetamide at meta-position of ring C having methoxy substitution ortho to it provided favorable activity profile (**9a-k** series). Comparison of compounds carrying substitution on the phenyl ring of oxy-acetamide side chain (**9b-j**) with its unsubstituted counterpart (**9a**) revealed (i) electron-donating group (methoxy) at *ortho*-position is favorable for potent and selective inhibition of CYP1B1 and (ii) electron-withdrawing group (fluro) at *para*-position is favorable for potent and selective inhibition of CYP1A1.

Molecular Modelling. CYP enzymes are part of a biological hydroxylation machinery responsible for Phase I hydroxylation reactions observed in drug metabolism. They confer

hydroxylation of substrate through sequential events involving electron transfer. The inhibitors designed were supposed to displace the water molecule in CYP enzymes and disrupt the formation of heme-oxo intermediate between the substrate, heme and CYP enzyme. Molecular modelling studies at the substrate binding site indicate that both rings of quinazoline-2-one nucleus display π-π interactions with the Phe 231 residue in F-helix. This is one of the crucial hydrophobic interactions required for inhibition of CYP1 family isoforms (Wang et al., 2011; Walsh et al., 2013). The higher potency of **9b** over **7b** for CYP1B1 inhibition could be justified due to the presence of the additional π-π interactions with the Phe-134 residue. Besides this, the chromene nucleus of ANF display strong H-bonding with the anionic charged Asp 333 residue (distance is 2.76 Å) in I helix. In case of **7b** and **9b**, we were able to mimic these interactions through C-2 carbonyl group with the distance of < 3 Å. The OMe group of the terminal ring was present in close proximity to heme and the linker chain interacts by favorable van der Waal's interactions with the residue lining the binding cavity. These residues include Asp 326, Val 395, Asp 333, Thr 510, Asn 228 and Phe 268 (Figure 4A). The phenyl ring attached linker -OCH_2CONH- offers flexibility in the molecule and thus terminal 2-methoxyphenyl ring can adopt multiple ring conformations at amide linkages in **7b** and **9b**. This flexibility of 2-methoxy phenyl ring in **7b** lead to folding of ring conformation in such a way that the **7b** linker obtains direct access to the deep pocket where NH group is in close vicinity to the heme metal atom. However, surprisingly in case of **9b** (with isovanillin attached linker), the amide bond flexibility allowed the 2-methoxy group of terminal phenyl ring to interact with the heme atom (distance is 2.33 Å) as shown in Figure 4B. The close and open conformations of the 2-methoxy phenyl ring at amide linkage are shown in overlaid images of **7b** and **9b** in substrate binding site of CYP1B1 (Figure 4C).

Specificity against Various CYP Isoforms. The most potent CYP1B1 inhibitors **7b** and **9b** along with few more inhibitors, identified in the human live cell assays using recombinant HEK293S cells, were screened for selectivity against CYPs 1A2, 2C9, 2C19, 2D6 and 3A4. The results, summarized in Table 5, indicate that none of the compounds show significant inhibitory activity against CYP 2 and 3 enzymes. Importantly, the compounds **7b**, and **9b** had IC_{50} values greater than 10 μM for inhibition of the CYP2 and CYP3 enzymes. This indicates that both pairs of compounds are highly selective towards CYP1A1 and CYP1B1. The rationale for higher selectivity of **7b** and **9b** for CYP1B1 was also studied by aligning the binding site of CYP2 and CYP3 family isoforms to CYP1B1. The CYP2 and CYP3 family enzymes such as 2D6 and 3A4 have large open binding site which is highly flexible so that it could accommodate a wide range of substrates. Most of the CYP2D6 and CYP3A4 inhibitors act by ionic charge-charge interactions, which are missing in the case of compounds **7b**, and **9b,** as shown in Figures S13 and S14 of Supporting Information.

Validation of the Best CYP1A1/CYP1B1 Inhibitors Identified in CYP1-expressing HEK293 Cells, via Cell Cycle Analyses

Rescue from Benzo[*a*]pyrene's Toxicity in CYP1A1-expressing Human Lung Fibroblast WI-38 Cells, by CYP1A1 Inhibitors. Transformed cancer cell lines have been used to study cellular responses to carcinogens (Calabrese, 2005). However, these cells do not reflect the physiological status of normal tissues. Hence, CYP1A1-overexpressing human lung normal fibroblast cells, WI-38, have been exposed to the pro-carcinogen benzo[*a*]pyrene, B[*a*]P, to address the question whether these cells would metabolize B[*a*]P to a carcinogenic product (e.g. benzo[*a*]pyrene diol epoxide; BPDE) that would form an adduct with DNA which would block cell growth. As shown in Table 6, the EC_{50} of B[*a*]P

was significantly lowered (EC_{50} = 0.8 µM) in the CYP1A1-expressing cell line, WI-38::pcDNA3.1/CYP1A1 (i.e. WI-38 cells stably transfected with the plasmid pcDNA3.1/CYP1A1), compared to WI-38 cells transfected with the empty plasmid, pcDNA3.1 (EC_{50} = 17.2 µM). This would indicate that B[*a*]P manifests toxicity only in cells which express CYP1A1. After that, the CYP1A1-overexpressing WI-38 cells were first pre-treated with the CYP1A1 inhibitors, identified in HEK293S recombinant cell assay, and then the B[*a*]P induced toxicity was measured after addition of B[*a*]P to the cells. As depicted in Table 7, the potent CYP1A1 inhibitor **9i** was able to reverse completely B[*a*]P's toxicity in WI-38::pcDNA3.1/CYP1A1 cells (the EC_{50} value of B[*a*]P was back to 17.0 µM). Similarly, the other CYP1A1 inhibitors **7g** and **9c** were also able to reverse B[*a*]P's toxicity. With the compounds that were less active in their inhibition of CYP1A1 (e.g. compounds **7c** and **7e**), in the HEK293S-cell-assay, less reversal in the toxicity of B[*a*]P was observed.

The effect of CYP1A1 inhibitors on the cell cycle, in the presence of B[*a*]P, was investigated by first pre-treating CYP1A1-expressing WI-38 cells with the most potent CYP1A1 inhibitors, compounds **7g** or **9i**, and then exposing the cells to B[*a*]P. CYP1A1 metabolizes B[*a*]P to its diol-epoxide (BPDE) and corresponding *o*-quinone which intercalate DNA and thereby should block cells primarily at the S phase of the cell division cycle. It has been suggested that formation of this DNA adduct causes mutations in DNA that ultimately leads to the onset of cancer (Moorthy et al., 2015; Androutsopoulos et al., 2009).

Upon exposure of CYP1A1-expressing WI-38 normal fibroblast cells (Figure 5A) to an EC_{50} concentration of B[*a*]P for 3 h and then releasing cells into fresh medium for 57 h, the cells did face a block at the S phase of the cell cycle (Figure 5B). This would be expected if the CYP1A1 protein (Figure 5E), expressed within WI-38 cells, were to be a functional enzyme. However, when cells were at first pre-incubated for 20 h with a CYP1A1-specific

inhibitor, for example, compounds **7g** or **9i** at their IC_{50} concentrations (0.06 μM and 0.03 μM, respectively), and then treated with an EC_{50} concentration of B[*a*]P for 3 h, followed by release into fresh medium, the cells did not anymore undergo an S phase block (Figures 5C and 5D). In fact, the cells re-entered the cell cycle as if the cells had not undergone any treatment with B[*a*]P. This implied that the CYP1A1-mediated metabolism of B[*a*]P must have been prevented by compounds **7g** and **9i**, demonstrating that, in the cellular context, they were indeed true inhibitors of the CYP1A1 enzyme.

In summary, we have identified two potent inhibitors of CYP1A1 (compounds **7g** and **9i**), using recombinant HEK293S cells, which have IC_{50} values of 60 nM and 30 nM, respectively. This would not have been possible if we had relied only on recombinant microsomal CYP1A1 enzymes.

Reversal of Cisplatin Resistance by CYP1B1 Inhibitors. Since it has been reported that inactivating CYP1B1 polymorphisms modify the risk towards the onset of prostate (Gajjar et al., 2012; Li et al., 2015), lung (Lao et al., 2014) pancreatic (Vrana et al., 2010) and colon cancers (Mei et al., 2012), stable CYP1B1-expressing human cancer cells PC-3/prostate (p53-null), COR-L23/lung (p53-mutant), MIAPaCa-2/pancreatic (p53-mutant), LS174T/colon (p53-positive but Bax-null) cells were constructed to investigate if the CYP1B1 inhibitors, identified in the HEK293S-cell-assay, were able to overcome cisplatin resistance in these cells (Mohd Siddique et al., 2016; Mohd Siddique et al., 2017). The four cell lines overexpressing CYP1B1 protein were constructed via stable transfection of the plasmid pcDNA3.1/CYP1B1 (Mohd Siddique et al., 2016; Mohd Siddique et al., 2017). The EC_{50} values of cisplatin, in each cell line, were determined (Table 8). The cisplatin EC_{50} values increased dramatically, from 3-4.5 μM to 50-90 μM, when CYP1B1 was stably expressed in these four-different cancer cell types (Figure 6). When the CYP1B1-overexpressing stable

cells were pre-treated for 24 h with one of the CYP1B1 inhibitors, identified in the HEK293S-cell-assay, the resistance to cisplatin was overcome (Table 9). For example, for compound **9b** which is a potent inhibitor of CYP1B1 enzyme, the EC_{50} value of cisplatin reversed back to 2.7 μM from 50 μM in PC-3 cells transfected with CYP1B1 plasmid (Table 9).

Expression of the CYP1B1 protein in the four cell lines PC-3, COR-L23, MIAPaCa-2 and LS174T, stably transfected with the plasmid pcDNA3.1/CYP1B1 (Mohd Siddique et al., 2016; Mohd Siddique et al., 2017), were confirmed by Western blotting (Figure 6).

The EC_{50} values of cisplatin in the four CYP1B1 overexpressing cell lines, in the presence of the most potent CYP1B1 inhibitor, compound **9b**, is depicted graphically in Figure 7. Cells were pre-treated with compound **9b**, for 24 h, before treatment with cisplatin for 3 h followed by release of cells into fresh medium for 33 h. The EC_{50} graphs for compound **9b**, after testing it in the four cancer cell lines PC-3, COR-L23, MIAPaCa-2 and LS174T, indicated that there is a dramatic decrease of cisplatin's EC_{50} values when cells were pre-incubated with the CYP1B1-specific inhibitor compound **9b**.

A consequence of treating PC-3, COR-L23, MIAPaca-2 or LS174T cells with cisplatin would be that they would become arrested at the G_2/M phase of the cell cycle (Eastman, 1987). As expected, MIAPaca-2::pcDNA3.1/CYP1B1 pancreatic cells, stably transfected with the plasmid encoding the human CYP1B1 gene, indeed did arrest at G_2/M (Figure 8A). This G_2/M block is seen as a protective mechanism that enables cells to pause and repair cisplatin-damaged DNA before crossing the threshold of mitosis (Aguda, 1999).

After this observation, MIAPaCa-2::pcDNA3.1/CYP1B1 pancreatic cells were pre-incubated (at 2x IC_{50} concentrations) with the four CYP1B1-specific inhibitors, compounds

5e, **7b**, **7c** and **9b**, for 24 h, before cells were treated with EC_{50} concentrations of cisplatin, which had been determined in the presence of 2x IC_{50} concentrations of inhibitors (Table 9), for 3 h. The results clearly show that, after release of CYP1B1-inhibited cells into fresh medium for 33 h, the cells no more suffered a G_2/M block but progressed further into the cell cycle and underwent between 17% to 35% of apoptosis as indicated by the sub-G_1 peaks (in Figures 8B to 8E). This established that the CYP1B1-expressing cells were being re-sensitized to cisplatin in the presence of the potent CYP1B1 inhibitors identified in the live HEK293S-cell-assay.

Compound **9b** was the most potent CYP1B1 inhibitor identified in the HEK293S-cell-assay and had shown the highest levels of apoptosis in the experiment with MIAPaCa-2::pcDNA3.1/CYP1B1 cells which were treated first with compound **9b** and then with cisplatin (compare Figures 8B to 8D with Figure 8E). Hence, it was further tested in the three CYP1B1-expressing human cancer lines that were derived from the prostate (PC-3), lung (COR-L23) and colon (LS174T). The results again show that pre-incubation of cells with a CYP1B1-specific inhibitor, before exposing the recombinant CYP1B1-expressing cells (PC-3-1B1, COR-L23-1B1, LS174T-1B1) to cisplatin (CP), re-sensitizes the cells to cisplatin and induces a fair amount of apoptosis (i.e. 26-46%) as seen by the percentages of the sub-G_1 peaks (in Figures 9A to 9C). Cells were again pre-incubated with the CYP1B1-specific inhibitor **9b** (at 2 x IC_{50} concentration) for 24h. Like with MIAPaCa-1B1:: pcDNA3.1/CYP1B1 cells, the human CYP1B1 gene-bearing derivatives of the three cell lines PC-3-1B1, COR-L23-1B1 and LS174T-1B1 had shown mainly a G_2/M block (results not shown) on exposure to EC_{50} concentrations of cisplatin alone (i.e. 50, 63 and 90 µM, respectively; Table 8).

In summary, we have identified potent and selective inhibitors of CYP1B1, compounds **5e**, **7b**, **7c** and **9b** from a small chemical library of 27 compounds. Compound **9b** was the most potent, with an IC_{50} value of 21 nM, in live human HEK293S cells, which had been adapted to grow in 'suspension'. It displays highly selective inhibition of CYP1B1. Its CYP1B1 inhibitory activity was further validated by investigating its ability to overcome cisplatin resistance in four different cancer cell lines PC-3, COR-L23, MIAPaCa-2 and LS174T. The ability of compound **9b** to effectively overcome resistance to cisplatin, in four different cancer cell lines which overexpress CYP1B1, warrants its further investigation in preclinical studies.

CONCLUSIONS

This study has shown that the human HEK293S-cell-assay system is unique, and that it is more reliable than the microsomal assays for the identification of CYP1 inhibitors. The human cell system may find wider use in pre-clinical studies that targets (i) the identification of the true inhibitors of CYP enzymes, which occur in vivo, with the aim of understanding, clarifying and predicting possible drug-drug interactions of a potential clinical entity, (ii) the identification and characterization of metabolites that are formed from CYP-mediated reactions in vivo, which are essential for embarking on clinical trials and (iii) the compounds that are difficult, at the moment impossible, to metabolize by hepatocytes which lose all CYP activity within 6 h of incubation at 37 ºC (Basu & Shaik, 2016).

This novel live cell technology has also the potential to define accurately the metabolic profiles of a large number of drug candidates, rapidly and reproducibly. It could be developed further to create tailor-made multiple CYP-expressing systems that are more akin to hepatocytes. Furthermore, with time and resources, 'stable' CYP-expressing HEK293S cells

could be obtained where CYP genes of clinical interest would be integrated into human cells' chromosomal loci. Currently each transfection, as described, allows the assaying of 250-300 compounds for inhibition of a CYP enzyme.

MATERIALS AND METHODS

General Information. All the chemicals were purchased from Spectro-Chem, Hi-media, Acros Organics or Sigma Aldrich. Solvents were purchased from Rankem and used as it was or otherwise specified accordingly. All the reactions were carried out under open air and in dried flask. Precoated silica gel aluminum plates (Merck) were used for reaction monitoring and visualized under UV light. Column chromatography was done using Merck silica gel (60-100 mesh). Carbon (^{13}C) and Proton (^{1}H) nuclear magnetic resonance (NMR) spectra were recorded on JEOL 400 MHz or Bruker 300 MHz instruments using dimethyl sulfoxide (DMSO-D6) solvent and tetramethylsilane as an internal standard (^{13}C NMR DMSO: δ 39.5, TMS: δ 0.00 ppm and ^{1}H NMR: DMSO δ 2.5 ppm).

Procedure for Synthesis of Intermediates 3, 6 and 8: Various substituted anilines were dissolved in glacial acetic acid at 0 °C, to this was added over 30 min choloroacetyl chloride (2 equivalents). The reaction mixture was brought to room temperature and stirred overnight. Saturated sodium bicarbonate solution was added till complete neutralization. The resulting precipitate was filtered off and washed with n-hexane and dried. The resultant product was used further without any purification. Either of 4-hydroxy benzaldehyde (**2a**), vanillin (**2b**) or isovanillin (**2c**) (1 equivalent) was dissolved in acetone and potassium carbonate (2 equivalents) was added. Then corresponding substituted acetamide (**1**) was mixed to the stirring solution. Finally, potassium iodide (1.5 equivalent) was added. The reaction mixture was refluxed for 8-10 hrs. After completion of reaction, the resultant mixture was

concentrated and treated with water and extracted with ethyl acetate (3 x 20 ml). The organic layers were combined and treated with brine and dried over sodium sulfate and concentrated. The crude mixture was purified over silica gel (60-120) using petroleum ether: ethyl acetate (9:1).

Procedure for the Synthesis of 5a-i, 7a-g and 9a-k. To the stirring solution of 2-aminobenzamide (4.1 equivalents) in dimethylformamide, sodium acetate (2 equivalents) was added. After stirring for 10 minutes the rare substituted benzaldehydes (**3, 6** and **8**, 1 equivalent) and iodine (2 equivalents) were added. The reaction mixture was heated at 70-80°C for 20-24 hrs. Then reaction mixture was poured on to crushed. The resulting mixture was treated with sodium thiosulphate (10% w/v in water) to reduce the remaining iodine. The precipitate was filtered off and washed with n-Hexane: Ethyl acetate (50:50).

N-cyclohexyl-2-(4-(4-oxo-3,4-dihydroquinazolin-2-yl)phenoxy) acetamide (5a): White powder, 1.214g (yield 87.5%); M.P.: 264-267°C; ^{1}H-NMR (400 MHz, DMSO-d_6) δ 1.20 (d, J = 10.4 Hz, 4H, C$\underline{H}_2$) 1.52 (d, J = 11.5 Hz, 1H, C$\underline{H}$), 1.64-1.69 (m, 4H, C$\underline{H}_2$), 2.46 (s, 3H, C$\underline{H}_2$), 4.52 (s, 2H, OC$\underline{H}_2$), 8.11-7.04 (m, 9H, ArH), 12.36 (s, 1H, CO-N$\underline{H}$); ^{13}C-NMR (101 MHz, DMSO-d_6) δ 25.48, 25.68, 32.79, 48.13, 67.45, 115.16, 116.44, 121.25, 126.37, 127.53, 129.98, 131.10, 134.90, 149.49, 160.83, 166.66. HRMS (ESI): m/z $[M+H]^+$ calculated 378.1818, found 378.1819

2-(4-(4-oxo-3,4-dihydroquinazolin-2-yl)phenoxy)-N-phenylacetamide (5b): White powder, 1.281g (yield 93.98%); M.P.: 252-253°C; Mass (M+1) Calculated 372.13, Found 372.2; ^{1}H NMR (400 MHz, DMSO-d6) δ 4.81 (s, 2H, OC$\underline{H}_2$), 8.18-7.07(m, 13H, Ar-$\underline{H}$), 10.15 (s, 1H, CO-N$\underline{H}$), 12.43 (s, 1H, CO-N$\underline{H}$). ^{13}C-NMR (101 MHz, DMSO-D_6) δ 67.62, 114.92, 117.64, 120.20, 124.21, 126.37, 128.80, 129.27, 129.98, 133.78, 134.62, 135.12, 138.91, 148.54, 152.35, 158.52, 160.94, 164.23, 166.97

2-(4-(4-oxo-3,4-dihydroquinazolin-2-yl)phenoxy)-N-p-tolylacetamide (5c): White powder, 1.401 g (Yield 98%); M.P.: 248-250°C; Mass (M+1) Calculated 386.15, Found 386.1; ^{1}H NMR (400 MHz, DMSO-d_6) δ 2.24 (s, 3H, Ar-C$\underline{H}_3$), 4.79 (s, 2H, OC$\underline{H}_2$), 8.18-7.13(m, 12H, Ar-H), 10.08 (s, 1H, CO-N$\underline{H}$), 12.42 (brs., 1H, CO-N$\underline{H}$); ^{13}C-NMR (101 MHz, DMSO-D6) δ 20.89, 67.52, 115.14, 120.15, 125.87, 126.27, 127.74, 129.57, 129.57, 129.87, 133.16, 135.06, 136.24, 149.33, 162.72, 166.34; HRMS (ESI): m/z [M+H]+ calculated 386.1505, found 386.1501

N-(3-chlorophenyl)-2-(4-(4-oxo-3,4-dihydroquinazolin-2-yl)phenoxy) acetamide (5d): White powder, 1.317g (yield 92.13%); M.P.: 252-254°C; Mass (M+1) Calculated 404.1, Found 404.2; ^{1}H NMR (400 MHz, DMSO-d_6) δ 4.83 (s, 2H, OC$\underline{H}_2$), 8.18-7.14 (m, 12H, Ar-$\underline{H}$), 10.35 (s, 1H, CO-N$\underline{H}$),12.43 (br. s, 1H, CO-N$\underline{H}$); ^{13}C-NMR (101 MHz, DMSO-D6) δ 67.47, 112.71, 115.19, 115.29, 118.55, 119.63, 121.17, 123.95, 126.02, 126.30, 126.69, 127.77, 127.85, 129.93, 130.96, 133.54, 135.04, 140.25, 149.35, 152.27, 160.79, 162.77, 167.09. HRMS (ESI): m/z $[M+H]^+$ calculated 406.0958, found 406.0951

N-(4-nitrophenyl)-2-(4-(4-oxo-3,4-dihydroquinazolin-2-yl)phenoxy) acetamide (5e): Yellowish orange powder, 0.674g (yield 87.96%); M.P.: 151-155°C; Mass (M+1) Calculated 417.11, Found 417.2; ^{1}H NMR (400 MHz, DMSO-d_6) δ 4.95 (s, 2H, OC$\underline{H}_2$), 8.18-7.17 (m, 12H, Ar-H), 9.86 (s, 1H, CO-N$\underline{H}$), 10.91 (s, 1H, CO-N$\underline{H}$); ^{13}C-NMR (101 MHz, DMSO-d_6) δ 67.44, 115.69, 119.35, 125.73, 130.56, 132.55, 143.29, 144.82, 163.23, 167.39, 191.95. HRMS (ESI): m/z $[M+H]^+$ calculated 417.1199, found 417.1198.

N-(4-ethoxyphenyl)-2-(4-(4-oxo-3,4-dihydroquinazolin-2-yl)phenoxy) acetamide (5f): White powder, 0.707g (yield 92.66%); M.P.: 102-104°C; Mass (M+1) Calculated 414.15, Found 414.3; ^{1}H NMR (400 MHz, DMSO-d_6) δ 1.29 (t, J = 6.85 Hz, 3H, C$\underline{H}_3$), 3.96 (q, J = 6.85 Hz, 2H, OC$\underline{H}_2$), 4.79 (s, 2H, OC$\underline{H}_2$), 7.88-6.86 (m, 12H, Ar-$\underline{H}$), 9.86 (s, 1H, CO-

N<u>H</u>), 10.01 (s, 1H, CO-N<u>H</u>); ^{13}C-NMR (101 MHz, DMSO-d_6) δ 14.7, 63.11, 114.40, 115.22, 121.34, 130.11, 131.28, 131.78, 162.80, 165.38, 191.38. HRMS (ESI): m/z $[M+H]^+$ calculated 416.161, found 416.1605.

N-(naphthalen-2-yl)-2-(4-(4-oxo-3,4-dihydroquinazolin-2-yl)phenoxy) acetamide (5g): Light brown powder, 1.22g (yield 83.5%); M.P.: 190-192 °C; Mass (M+1) Calculated 422.15, Found 422.2; ^{1}H NMR (400 MHz, DMSO-d_6) δ 4.89 (s, 2H, OC<u>H</u>$_2$), 8.26 - 7.06 (m, 15H, Ar-<u>H</u>), 10.37 (s, 1H, CO-N<u>H</u>), 12.44 (br. s., 1H, CO-N<u>H</u>); ^{13}C-NMR (101 MHz, DMSO-d_6) δ 67.62, 115.26, 116.42, 120.75, 121.24, 125.38, 126.00, 126.37, 126.76, 127.04, 127.89, 128.97, 129.99, 130.48, 133.84, 135.13, 136.47, 149.43, 152.46, 160.82, 162.83, 166.69. HRMS (ESI): m/z $[M+H]^+$ calculated 422.1505, found 422.1499

N-(naphthalen-1-yl)-2-(4-(4-oxo-3,4-dihydroquinazolin-2-yl)phenoxy) acetamide (5h): Cream powder, 0.913g (yield 59%); M.P.: 199-201°C; Mass (M+1) Calculated 422.15, Found 422.2; ^{1}H NMR (400 MHz, DMSO- d_6) δ 5.13 (s, 2H, OC<u>H</u>$_2$), 7.25 -8.00 (m, 13H, Ar-<u>H</u>), 9.89 (s, 1H, CO-N<u>H</u>), 10.23 (s, 1H, CO-N<u>H</u>); ^{13}C-NMR (101 MHz, DMSO- d_6) δ 67.62, 115.79, 122.92, 123.32, 126.09, 126.50, 126.67, 128.66, 130.65, 132.32, 133.27, 134.23, 163.34, 167.33, 191.95.

2-(4-(4-oxo-3,4-dihydroquinazolin-2-yl)phenoxy)-N-phenethyl acetamide (5i): White powder, 1.319g (yield 91%); M.P.: 252-253°C; Mass (M+1) Calculated 400.16, Found 400.2; ^{1}H-NMR (400 MHz, DMSO- d_6) δ 2.46 (q, J = 1.8 Hz, 2H, C<u>H</u>$_2$), 2.72 (t, J = 7.4 Hz, 2H, C<u>H</u>$_2$), 4.54 (s, 2H, OC<u>H</u>$_2$), 7.04-8.21 (m, 13H, Ar-<u>H</u>), 12.40 (s, 1H, CO-N<u>H</u>); ^{13}C-NMR (101 MHz, DMSO-d_6) δ 35.62, 40.90, 67.47, 115.26, 121.21, 125.93, 126.38, 126.67, 127.72, 128.89, 129.17, 129.97, 135.13, 139.79, 152.40, 160.81, 167.71. HRMS (ESI): m/z $[M+H]^+$ calculated 400. 1661, found 400.1655

(N-butyl-2-(2-methoxy-4-(4-oxo-3,4-dihydroquinazolin-2-yl)phenoxy) acetamide) (7a): Yellowish powder, 0.607g (yield 88.5%); M.P.: 185-186°C; (M+1) Calculated 381.17, Found 382.1; ^{1}H NMR (400 MHz, DMSO- d_6) δ 0.85 (3 H, t, *J*= 7.24 Hz, C$\underline{H}_3$), 1.25 (2 H, m, C$\underline{H}_2$), 1.39 (2 H, m, C$\underline{H}_2$), 3.11 (2 H, q, *J*=6.58 Hz, C$\underline{H}_2$), 3.89 (3 H, s, OC$\underline{H}_3$), 4.55 (2 H, s, OC$\underline{H}_2$), 7.01-8.07 (m, 7H, Ar-$\underline{H}$), 8.38 (1 H, s, CO-N$\underline{H}$), 12.57 (1 H, br. s, CO-N$\underline{H}$). HRMS (ESI): m/z $[M+H]^+$ calculated 382.1767, found 382.1759

2-(2-methoxy-4-(4-oxo-3,4-dihydroquinazolin-2-yl)phenoxy)-N-(2- methoxy phenyl) acetamide (7b). White powder, 0.268g (yield 84.54%); (M+1) Calculated 532.16, Found 432.08; M.P.: 253-255°C; ^{1}H NMR (400 MHz, DMSO-D6) δ 3.864 (s, 3H, OC$\underline{H}_3$), 3.93 (s, 3H, OC$\underline{H}_3$), 4.803 (s, 2H, OC$\underline{H}_2$), 6.883-8.353 (m, 11H, Ar-$\underline{H}$) 9.286 (s, 1H, CO-N$\underline{H}$), 12.585 (s, 1H, CO-N$\underline{H}$); ^{13}C-NMR (101 MHz, DMSO-D6) δ 56.48, 68.36, 111.55, 113.83, 120.39, 121.05, 121.71, 124.96, 126.38, 127.10, 134.53, 143.42, 149.13, 149.23, 166.40. HRMS (ESI): m/z $[M+H]^+$ calculated 432.1559, found 432.1559

2-(2-methoxy-4-(4-oxo-3,4-dihydroquinazolin-2-yl)phenoxy)-N-(3-methoxyphenyl) acetamide (7c): White powder, 0.263g (yield 82.96%); ^{1}H NMR (400 MHz, DMSO- d_6) δ 3.71(s, 3H, OC$\underline{H}_3$), 3.86 (s, 3H, OC$\underline{H}_3$), 4.75 (s, 2H, OC$\underline{H}_2$), 6.85-8.34 (m, 11H, Ar-$\underline{H}$), 9.994 (s, 1H, -CO-N$\underline{H}$), 12.40 (s, 1H, -CO-N$\underline{H}$); ^{13}C-NMR (101 MHz, DMSO- d_6) δ 55.80, 56.38, 68.82, 112.37, 113.77, 114.43, 121.70, 122.63, 125.21, 126.39, 126.75, 131.81, 135.13, 147.79, 152.43, 156.11, 166.44.

2-(2-methoxy-4-(4-oxo-3,4-dihydroquinazolin-2-yl)phenoxy)-N-(4-methoxyphenyl) acetamide (7d): White powder, 1.234 g (yield 77. 91%); M.P.: 161-163°C; Mass (M+1): Calculated 432.15, Found 432.2; ^{1}H NMR (400 MHz, DMSO- d_6) δ 3.70 (s, 3H, OC$\underline{H}_3$), 3.86 (s, 3H, OC$\underline{H}_3$),4.80 (s, 2H, OC$\underline{H}_2$), 7.76-6.88 (m, 11H, Ar-$\underline{H}$), 9.83 (s, 1H, -CO-N$\underline{H}$), 10.04 (s, 1H, CO-N$\underline{H}$); ^{13}C-NMR (101 MHz, DMSO- d_6) δ 55.64, 56.11, 68.21, 110.59, 113.28,

114.39, 121.49, 126.07, 130.75, 131.91, 149.80, 153.29, 156.00, 165.78, 191.88. HRMS (ESI): m/z $[M+H]^+$ calculated 432.1559, found 432.1553

N-(4-ethoxyphenyl)-2-(2-methoxy-4-(4-oxo-3,4-dihydroquinazolin-2-yl) phenoxy) acetamide (7e): White powder, 1.414g (yield 86.43%); M.P.: 150-152°C; Mass (M+1) Calculated 446.17 Found 446.2; ^{1}H NMR (400 MHz, DMSO- d_6) δ 1.300 (t, *J* = 7.2Hz, 3H, C<u>H</u>$_3$), 3.856 (s, 3H, OC<u>H</u>$_3$), 3.983-3.931 (q, 2H, OC<u>H</u>$_2$),4.792(s, 2H, OC<u>H</u>$_2$), 7.530-6.870 (m, 11H, Ar-<u>H</u>), 9.830 (s, 1H, CO-N<u>H</u>), 10.015 (s, 1H, CO-N<u>H</u>); ^{13}C-NMR (101 MHz, DMSO- d_6) δ 15.12, 56.1, 63.56, 68.21, 110.58, 113.28, 114.91, 121.46, 126.08, 130.75, 131.81, 149.80, 153.30, 155.25, 165.76, 191.88. HRMS (ESI): m/z $[M+H]^+$ calculated 446.1716, found 446.1711

N-(4-fluorophenyl)-2-(2-methoxy-4-(4-oxo-3, 4-dihydroquinazolin-2-yl)phenoxy) acetamide (7f): Yellowish powder, 1.412g (Yield 91.6%); M.P.: 135-138°C; (M+1) Calculated 420.13, Found 420.2; ^{1}H NMR (400 MHz, DMSO- d_6) δ 3.827 (s, 3H, OC<u>H</u>$_3$), 4.827 (s, 2H, OC<u>H</u>$_2$), 7.626-7.09 (m, 10H, Ar-<u>H</u>), 9.831, (s, 1H, CO-N<u>H</u>),10.241 (s, 1H, CO-N<u>H</u>); ^{13}C-NMR (101 MHz, DMSO- d_6) δ 56.11, 68.10, 110.61, 113.30, 115.75, 115.97, 121.69, 121.77, 126.06, 130.79, 135.22, 149.79, 153.23, 157.50, 159.89, 166.25, 191.89. HRMS (ESI): m/z $[M+H]^+$ calculated 420.136, found 420.1265

2-(2-methoxy-4-(4-oxo-3,4-dihydroquinazolin-2-yl)phenoxy)-N-(naphthalen-2-yl) acetamide (7g): White powder, 1.31g (yield 82.28%); M.P.: 232-235°C; Mass (M+1) Calculated 452.16 Found 452.2; ^{1}H NMR (400 MHz, DMSO- d_6) δ 3.91 (s, 3H, OC<u>H</u>$_3$), 4.84 (s, 2H, OC<u>H</u>$_2$), 7.09-8.27 (m, 14H, Ar-<u>H</u>), 10.34 (s, 1H, CO-N<u>H</u>), 12.46 (s, 1H, CO-N<u>H</u>); ^{13}C-NMR (101 MHz, DMSO- d_6) δ 56.36, 68.41, 111.78, 113.76, 116.19, 120.54, 121.22, 121.47, 125.37, 126.30, 127.07, 127.88, 129.05, 130.46, 133.86, 135.16, 136.60, 149.32, 150.62, 152.30, 162.80, 167.01.

2-(2-methoxy-5-(4-oxo-3,4-dihydroquinazolin-2-yl)phenoxy)-N-phenyl acetamide (9a): White powder, 1.314g (yield 89.14%); M.P.: 227-229°C; (M-1) Calculated 400.40, Found 400.3; ^{1}H-NMR (400 MHz, DMSO- d_6) δ 3.86 (s, 3H, OC<u>H</u>$_3$) 4.78 (s, 2H, OC<u>H</u>$_2$), 7.04-8.33 (m, 12H, Ar-<u>H</u>), 10.08 (s, 1H, CO-N<u>H</u>), 12.46 (d, J = 52.8 Hz, 1H, CO-N<u>H</u>); ^{13}C-NMR (101 MHz, DMSO- d_6) δ 56.38, 68.87, 112.38, 113.76, 120.07, 124.25, 126.60, 127.77, 129.36, 134.67, 138.89, 143.42, 147.68, 161.30, 162.74, 167.12. HRMS (ESI): m/z $[M+H]^+$ calculated 402.1454, found 402.1448

2-(2-methoxy-5-(4-oxo-3,4-dihydroquinazolin-2-yl)phenoxy)-N-(2-methoxy phenyl) acetamide (9b): White powder, 0.252g (yield 79.49%); M.P. 254.5-257°C; Mass (M+1) Calculated 432.15 found 432.15; ^{1}H NMR (400 MHz, DMSO- d_6) δ 3.85 (s, 6H, 2 x OC<u>H</u>$_3$), 4.818 (s, 2H, OC<u>H</u>$_2$), 6.904-8.338 (m, 11H, Ar-<u>H</u>), 9.275 (s, 1H, CO-N<u>H</u>), 12.392 (s, 1H, CO-N<u>H</u>); ^{13}C-NMR (101 MHz, DMSO- d_6) δ 56.49, 56.60, 68.60, 111.81, 112.47, 113.53, 121.06, 123.02, 124.92, 125.24, 126.37, 127.09, 127.84, 135.23, 147.00, 148.95, 152.02, 162.85, 166.74. HRMS (ESI): m/z $[M+H]^+$ calculated 432.1559, found 432.1551

2-(2-methoxy-5-(4-oxo-3,4-dihydroquinazolin-2-yl)phenoxy)-N-(3-methoxy phenyl) acetamide (9c): Light brown powder, 0.587g (yield 92.7%); M.P.: 114-117°C; Mass (M+1) Calculated 432.15, found 432.10; ^{1}H NMR (400 MHz, DMSO- d_6) δ 3.710 (s, 3H, OC<u>H</u>$_3$), 3.904 (s, 3H, OC<u>H</u>$_3$), 4.764 (s, 2H, OC<u>H</u>$_2$), 6.639 -7.606 (m, 10H, Ar-<u>H</u>), 9.804 (s, 1H, CO-N<u>H</u>), 10.108 (s, 1H, CO-N<u>H</u>); ^{13}C-NMR (101 MHz, DMSO- d_6) δ 55.52, 56.54, 68.27, 105.70, 109.62, 111.68, 112.16, 127.68, 130.18, 140.08, 148.50, 155.20, 160.06, 166.75, 191.83. HRMS (ESI): m/z $[M+H]^+$ calculated 432.1559, found 432.1552

2-(2-methoxy-5-(4-oxo-3,4-dihydroquinazolin-2-yl)phenoxy)-N-(4-methoxyphenyl) acetamide (9d): White powder, 1.387g (yield 87%); M.P.: 239-240°C; Mass (M+1) Calculated 432.15, Found 432.2; ^{1}H-NMR (400 MHz, DMSO- d_6) 3.68 (s, 3H, OC<u>H</u>$_3$), 3.88

(s, 3H, OC<u>H</u>$_3$), 4.71 (s, 2H, OC<u>H</u>$_2$), 6.86-7.57 (m, 11H, Ar-<u>H</u>), 9.78 (s, 1H, CO-N<u>H</u>), δ 9.97 (s, 1H, CO-N<u>H</u>). HRMS (ESI): m/z $[M+H]^+$ calculated 432.1559, found 432.1554

N-(4-ethoxyphenyl)-2-(2-methoxy-5-(4-oxo-3,4-dihydroquinazolin-2-yl)-phenoxy) acetamide (9e)*:* White powder, 1.469g (yield 92.73%); M.P.: 251-253°C; Mass (M+1) Found 448.1; ^{1}H NMR (400 MHz, DMSO- d$_6$) δ 2.72 (t, *J* = 7.09 Hz, 3H, OC<u>H</u>$_3$), 3.33 - 3.39 (m, 2H, OC<u>H</u>$_2$),3.83 (s, 3H, OC<u>H</u>$_3$), 4.58 (s, 2H, OC<u>H</u>$_2$), 6.98-7.49 (m, 11H, Ar-<u>H</u>), 8.03(s, 1H, CO-N<u>H</u>) 9.84 (s, 1H, CO-N<u>H</u>); ^{13}C-NMR (101 MHz, DMSO- d$_6$) δ 14.68, 55.78, 63.08, 68.33, 111.75, 113.28, 114.40, 121.16, 126.04, 127.26, 131.35, 134.40, 147.32, 151.73, 154.78, 162.43, 166.00. HRMS (ESI): m/z calculated 446.1716, found 446.1712 $[M+H]^+$,

2-(2-methoxy-4-(4-oxo-3,4-dihydroquinazolin-2-yl)phenoxy)-N-o-tolyl acetamide (9f): Cream powder, 0.507g (yield 82.97%); M.P.: 124-127 °C; Mass (M+1) Calculated 416.16, found 416.10; ^{1}H NMR (400 MHz, DMSO- d$_6$) δ 2.204 (s, 3H, C<u>H</u>$_3$), 3.87 (s, 3H, OC<u>H</u>$_3$), 4.872 (s, 2H, OC<u>H</u>$_2$), 7.08-7.55 (m, 11H, Ar-<u>H</u>), 9.392 (s, 1H, CO-N<u>H</u>), 9.851 (s, 1H, CO-N<u>H</u>); ^{13}C-NMR (101 MHz, DMSO- d$_6$) δ 18.07, 39.38, 39.59, 39.80, 40.01, 40.22, 40.43, 40.63, 56.21, 68.03, 110.54, 113.65, 124.57, 125.82, 126.18, 126.68, 130.93, 135.86, 149.85, 153.05, 166.18, 192.01.

N-(2-chlorophenyl)-2-(2-methoxy-5-(4-oxo-3,4-dihydroquinazolin -2-yl)-phenoxy) acetamide (9g): Yellowish powder, 1.296g (yield 81.05%); M.P.: 227-229°C; (M+1) Calculated 436.10, Found 436.10; ^{1}H NMR (400 MHz, DMSO- d$_6$) δ 3.867 (s, 3H, OC<u>H</u>$_3$), 4.876 (s, 2H, OC<u>H</u>$_2$), 7.143-8.035 (m, 11H, Ar-<u>H</u>), 9.564 (s, 1H, CO-N<u>H</u>), 12.406 (s, 1H, CO-N<u>H</u>); ^{13}C-NMR (101 MHz, DMSO- d$_6$) δ 56.46, 68.47, 112.40, 113.58, 122.94, 124.32, 125.22, 126.39, 127.80, 128.34, 130.03, 134.57, 135.17, 147.11, 149.37, 152.28, 162.86, 167.32. HRMS (ESI): m/z $[M+H]^+$ calculated 436.1064, found 436.1057

N-(4-chlorophenyl)-2-(2-methoxy-5-(4-oxo-3,4-dihydroquinazolin-2-yl) phenoxy) acetamide (9h): Light brown powder, 0.662g (yield 82.86%); M.P.: 229°C; (M+1) Calculated 436.10, Found 436.10; ^{1}H NMR (400 MHz, DMSO-d_6) δ 3.879 (s, 3H, OC<u>H</u>$_3$); 4.820 (s, 2H, OC<u>H</u>$_2$), 8.109-7.71(m, 11H, Ar-<u>H</u>), 10.32 (s, 1H, CO-N<u>H</u>), 12.71 (s, 1H, CO-N<u>H</u>); ^{13}C-NMR (101 MHz, DMSO- d_6) δ 56.33, 68.76, 112.37, 113.68, 121.62, 125.14, 126.31, 127.70, 127.78, 129.18, 137.79, 147.64, 167.15. HRMS (ESI): m/z $[M+H]^+$ calculated 436.1064, found 436.1061

N-(4-fluorophenyl)-2-(2-methoxy-5-(4-oxo-3,4-dihydroquinazolin-2-yl) phenoxy) acetamide (9i): White powder, 1.41g (yield 91.5%); M.P.: 124-126°C; ^{1}H NMR (400 MHz, DMSO- d_6) δ 3.898 (s, 3H, OC<u>H</u>$_3$); 4.792 (s, 2H, OC<u>H</u>$_2$), 7.810-7.114(m, 10H, Ar-<u>H</u>),9.779 (s, 1H, CO-N<u>H</u>),10.364 (s, 1H, CO-N<u>H</u>), ^{13}C-NMR (101 MHz, DMSO- d_6) δ 39.39, 39.59, 39.80, 40.01, 40.22, 40.43, 40.63, 56.44, 68.22, 111.83, 112.33, 118.61, 119.49, 123.93, 127.68, 131.09, 133.95, 140.53, 148.41, 154.80, 167.00, 191.83. HRMS (ESI): m/z $[M+H]^+$ calculated 420.136,found 419.9925

2-(2-methoxy-5-(4-oxo-3,4-dihydroquinazolin-2-yl)phenoxy)-N-(4-nitro phenyl) acetamide (9j): Yellowish powder, 0.279g (yield 85%); M.P.: 269-272°C; Mass (M+1) Calculated 447.13, Found 447.10; ^{1}H-NMR (400 MHz, DMSO- d_6) δ 3.86 (s, 3H, OC<u>H</u>$_3$), 4.86 (s, 2H, OC<u>H</u>$_2$), 7.14- 8.33 (m, 11H, Ar-<u>H</u>), 10.75 (s, 1H, -CO-N<u>H</u>), 12.52 (s, 1H, -CO-N<u>H</u>); ^{13}C-NMR (101 MHz, DMSO- d_6) δ 56.62, 68.68, 112.45, 113.74, 119.73, 122.86, 124.92, 125.59, 134.67, 143.02, 143.41, 145.28, 147.65, 152.51, 168.03. HRMS (ESI): m/z $[M+H]^+$ calculated 447.1305, found 447.1275

N-butyl-2-(2-methoxy-5-(4-oxo-3,4-dihydroquinazolin-2-yl)phenoxy) acetamide (9k): Cream colored powder, 0.236 g (yield 84.61%); M.P.: 194-197°C; Mass (M+1) Calculated 382.17, Found 382; ^{1}H NMR (400 MHz, DMSO- d_6) δ 0.759 (t, 3H, *J*= 6.8Hz, -

C<u>H</u>$_3$), 1.183 (m, 2H, -C<u>H</u>$_2$), 1.362 (m, 2H, -C<u>H</u>$_2$), 3.107 (q, 2H, 6.8Hz, -C<u>H</u>$_2$), 3.871 (s, 3H, -OC<u>H</u>$_3$), 4.593 (s, 2H, -OC<u>H</u>$_2$), 6.671-7.89 (m, 8H, Ar-<u>H</u>), 8.123 (s, 1H, -CO-N<u>H</u>), 12.39 (s, 1H, -CO-N<u>H</u>); ^{13}C-NMR (101 MHz, DMSO- d_6) δ 14.12, 19.89, 31.72, 56.48, 68.84, 112.35, 113.88, 119.49, 122.66, 125.23, 126.37, 126.75, 135.11, 137.03, 140.36, 147.65, 152.43, 167.93, 170.33. HRMS (ESI): m/z $[M+H]^+$ calculated 382.1767, found 382.1761.

Screening of Compounds Using Microsomal Enzymes Isolated from Recombinant Cells. The microsomal CYP enzymes, Bactosomes™, Sacchrosomes™ and Supersomes™, used in this study were manufactured by Cypex, CYP Design and Corning. The CYP enzymes, isolated from recombinant cells, were used to evaluate the percentage inhibition of a CYP by a compound and determine the IC_{50} values (the concentration at which 50% of the enzyme activity is inhibited) of a compound. Protocols for the use of Sacchrosomes have been published (Horley et al., 2017; Mohd Siddique et al., 2016; Mohd Siddique et al., 2017; Joshi et al., 2017). Protocols for the use of Bactosomes and Supersomes were provided by the manufacturers of the enzymes. Both percentage inhibition and IC_{50} values effectively reflect the inhibitory potential of a compound and normally hint at the possible effectiveness of a compound in a biological process. Percentage inhibition is determined at a specific concentration of a compound which is usually 10 µM. An assay which determines IC_{50} values of CYP enzymes includes the microsomes that bear the CYP enzymes, a chosen chemical compound in six serial dilutions in DMSO (with DMSO concentration never exceeding 0.5%), 96-well flat-bottomed microtiter plates, substrates such as 7-ER (7-ethoxyresorufin) or CEC (3-cyano-7-ethoxycoumarin) or EOMCC (7-ethoxy-methyloxy-3-cyanocoumarin) or DBF (dibenzylfluorescein), depending on the CYP enzyme used in the assay. The substrates form fluorescent products upon CYP metabolism. A fluorescent plate reader is used to monitor fluorescence emitted which ultimately determines IC_{50} values via measurement of fluorescence units at each endpoint (i.e. at each concentration of compound used). It is

perhaps obvious that some of the compounds can be fluorescent; therefore, the values obtained in wells that contained only compounds but no enzyme were subtracted from the values obtained in wells which contained enzyme and compound. Detailed procedures for enzyme inhibition studies is provided in our previous publications (Horley et al., 2017; Mohd Siddique et al., 2016; Mohd Siddique et al., 2017; Joshi et al., 2017; Mahale et al., 2014; Mahale et al., 2015) and sections associated with supporting information. All experiments were performed independently in triplicate.

Adaptation of Adherent HSK293 Cells for Growth in 'Suspension' to Obtain HEK293S Cells. Adherent HEK293 cells were obtained from ATCC (# CRL-1573). These cells were adapted for growth in 'suspension' by growing them initially in EMEM with 10% FBS (Sigma #M8028). After 3-4 subcultures, cells were mycoplasma-tested using Lookout mycoplasma PCR kit (Sigma #MP0035). Low passage cells (with >90% viability using trypan blue dye exclusion), in mid-exponential growth phase, were adapted to 'suspension' culture (Macallister et al., 1999) in serum-free medium (Invitrogen #12309-09). Cells (1 x 10^5 per mL) in 30 mL serum-free medium were adapted for 'suspension' growth in 125 mL EML polycarbonate flasks incubated at 37 °C, in the presence of 8% CO_2, and shaken at 130 rpm on a Sartorius orbital shaker. Cells in 'suspension' were sub-cultured regularly after cell counts reached 1 x 10^6 cells per mL and were monitored for viability and number of cell aggregates at each stage. Cells were considered fully adapted to 'suspension' when most cells were single and had acquired similar growth characteristics to that of parental adherent cells. Stocks of 'suspension' cells were frozen for further use. Frozen cells were sub-cultured twice before use in transfection of CYP gene-bearing expression plasmids.

Expression of CYP Gene Encoding Plasmids in HEK293S Cells. Actively dividing HEK293S cells (1x 10^6 per mL), in log phase, which showed >90% viability, via trypan blue

exclusion, were seeded in appropriate volumes in EML flasks and incubated at 37 °C, 8% CO_2, and shaken at 130 rpm on a Sartorius orbital shaker under 75% relative humidity. For transfection, endotoxin-free plasmids bearing the human genes coding for the CYP1A1, CYP1B1, CYP1A2, CYP2C9, CYP2C19, CYP2D6 and CYP3A4 proteins were used. Plasmid DNA-cationic lipid complexes were prepared as per manufacturer's (i.e. Invitrogen's) instructions in OptiPRO SFM reduced serum medium (Invitrogen, #12309-09). The ratio of DNA to cationic reagent was first optimized to achieve the best transfection efficiency. Aseptic preparations of DNA-lipid complexes were added slowly to the respective flasks containing HEK293S cells. The negative control was prepared by adding OptiPRO SFM reduced serum media to plasmid carrying no CYP gene insert. The plasmid that contains the gene that codes for the enhanced green fluorescent protein, eGFP, was used as a control to monitor transfection efficiency. HEK293S cells were incubated at 37 °C, with shaking, and checked for optimal expression of CYP enzymes at regular intervals. Cells were counted and viability was determined 24, 48, 72, 96 and 120 h post-transfection. For performing enzymatic assays, sufficient volumes of transfected cells were spun down at 200x g for 5 min at RT. The supernatants were discarded and the cells were washed once with pre-warmed Dulbeco's phosphate buffered saline without calcium and magnesium (DPBS; Gibco #14190-094). The cells were once again spun down at 200x g for 5 min and the cell pellets were gently re-suspended in pre-warmed growth media to obtain cell densities of 2-8 million cells per mL of transfected 'suspension' cells expressing different CYP enzymes. The cells, expressing individual CYPs, were tested for enzyme activity using a suitable fluorogenic substrate (see section, "Screening of Compounds Using Microsomal Enzymes Isolated from Recombinant Cells") and further validated using approved reference CYP-inhibitory compounds (Table 1).

Western Blotting. CYP expression in HEK293S cells was confirmed by Western blotting (Mahmood & Yang, 2012). HEK293 cells expressing CYPs were lysed in RIPA buffer (Sigma #RO278) containing AEBSF (4-(2-aminoethyl) benzenesulponyl fluoride-HCl; Melford #MB2003) as protease inhibitor (2 mM); total protein content in the lysates was quantified with the Pierce BCA protein assay kit (#23227). Proteins in cell lysates (around 5 µg) were separated on 10% SDS polyacrylamide gels by electrophoresis and transferred, by semi-dry method, to a PVDF membrane which was blocked for an hour at RT with 5% non-fatty milk (Bio-Rad, #1706404) solution in PBST (PBS containing 0.1% Tween). The membrane was then incubated with anti-CYP rabbit or mouse antibodies in 1% milk/PBST (1:500 or 1:1000) overnight at 4°C with gentle shaking. After 3 washes with PBST, membranes were incubated with goat anti-rabbit or anti-mouse HRP-tagged secondary antibodies (1:10000 or 1:20000) for 1h at RT. After further 3 washes with PBST, the immunoblots were developed using the enhanced luminol-based chemiluminescent *substrate* (ECL) substrate and the images were visualized using the ChemiDoc XRS system (Bio-Rad).

The following antibodies, used for confirming CYP expression, were procured from ProteinTech: CYP1A1 (#13241-1-A), CYP1A2 (#19936-1-AD), CYP1B1 (#18505), CYP2D6 (#17868-1-AP), CYP19A1 (#16554-1-AP), beta-actin (#60008-1-Ig). Antibodies for CYP3A4 (Corning #A254), CYP2C9 (Origene #TA503796), CYP2C19 (Abcam #22596-50) were from sources indicated.

Measuring CYP Enzyme Activities in Whole Live HEK293S Cells Using Fluorogenic Substrates. The activity of human CYP enzymes was evaluated in triplicates. Fluorogenic substrate solutions were prepared in 100% acetonitrile excepting 7-ER which was prepared in 100% DMSO. The final working stock of the FDA-approved CYP-specific inhibitors (Table 1) was prepared in pre-warmed DPBS or cell culture medium. The total reaction volume in

each well was 100 µL and the final concentration of organic solvents was maintained to <0.5%. The readout of CYP-based reactions, after addition of fluorogenic probes, was monitored on a fluorescence plate-reader (Biotek Synergy HT, software Gen version 5.0). The plates were read in kinetic mode for 60-120 min, in 1-2 min time intervals, at 37ºC. The linearity of the reaction, through product formation, was observed for each of the CYP reactions using suitable wavelengths for each of the products formed (Table 1). For each CYP assay, the number of cells/well was 100-300 x 10^3. The activity of HEK293S cells, carrying an empty plasmid, with no CYP gene insert acted as negative control. The net relative fluorescence counts (RFU) represent the rate of reaction for formation of products.

The reference FDA-approved CYP-inhibitory compounds were purchased from Sigma-Aldrich: ketoconazole (for CYP3A4; #K1003), furafylline (for CYP1A2; #F124), quinidine (CYP2D6; #Q3625), sulfaphenazole (CYP2C9; #S0758), ticlopidine (CYP2C19; #T16654), α-napthoflavone (for CYP1A1, CYP1A2, CYP1B1; #N5757).

All fluorogenic substrates for CYP activity studies were purchased from Sigma-Aldrich. They were dibenzylfluorescein (DBF, #D1791), 3-[2-(N,N-diethyl-N-methylammonium) ethyl]-7-methoxy-4-methylcoumarin (AMMC, #A1352), 7-benzyloxy-4-trifluoro-methylcoumarin (7-BFC, #B5057), 7-methoxy-4-trifluoromethyl-coumarin (7-MFC, #T3165C), 3-Cyano-7-ethoxycoumarin (CEC, #UC455), 7-ethoxy-resorufin (7-ER, #46121). The fluorescent products formed, upon reaction with CYPs, are indicated in the Figure legends.

CYP Inhibition in Whole HEK293S Cells by Reference Compounds and Screening of a Chemical Library. FDA-recommended CYP-inhibitory compounds were selected for validation of the CYP enzymes expressed within live HEK293S cells. For testing the compounds' inhibitory potential in CYP-expressing HEK293S cells, 100-300x 10^3 cells per

well were seeded in 50 µL volume in triplicates. The compounds either at single point concentration (10 µM), or at various concentrations (1 nM to 30 µM), for determination of IC_{50}, were added in 25 µL volume to the wells followed by incubation at 37°C, 8% CO_2, for 30 min. The fluorogenic substrates, in 25 µL, were then added to the wells and contents were mixed by shaking. The plate was read on the fluorescence plate-reader (Biotek Synergy HT) using suitable wavelengths as described in the Figure legends. The maximum change in relative fluorescence units (RFU) relative to negative control cells, containing empty plasmid, was calculated. The enzyme inhibition was plotted using sigmoidal curve (4 parameter variable slope equation) and half-inhibitory concentration (IC_{50}) values were analysed statistically using GraphPad Prism Software (Version 6.0). The IC_{50} values of CYP inhibitors were determined by fitting a non-linear curve of uninhibited fraction with incubation concentration of the inhibitors, using the following four-parameter model (Hill equation):

$$y = 1 - (\text{Bottom} + (\text{Top} - \text{Bottom})/(1 + (\text{IC50}/x)\text{^s})),$$

where Top denotes maximum inhibited fraction, Bottom denotes minimum inhibited fraction, 'S' is slope factor, 'x' is inhibitor concentration and 'y' denotes the uninhibited cells. The parameters Top and Bottom were limited between 0 and 1 by the GraphPad software.

To identify potential candidates that inhibit CYP1A1 or CYP1B1, screening of compound libraries at single point concentration (10 µM) was carried out. The potential hits identified from the initial screening were further taken for determination of IC_{50} values and dose-response studies.

Construction of Stable Cell Lines. After transfection of the CYP1A1 and CYP1B1 gene-bearing pcDNA3.1 plasmids, with the help of Amaxa-Nucleofector (following the manufacturers protocols), the transfectants were seeded onto a 100-mm tissue culture dish

(Corning) containing 8 mL of pre-warmed culture medium. After incubation for 2 days, the transfected cells were selected for G418 resistance in medium containing 1 mg/mL G418 (Gibco/BRL Life Technologies). After 10-15 days, the surviving single colonies (G418-resistant colonies) were picked up using cloning rings and transferred to 24-well dishes with further selection in medium containing 200 mg/mL G418. The expression of CYP enzymes, in G418-stabilized transfectants, were determined using immunocytochemistry and enzyme assays using fluorogenic substrate, 7-ethoxyresorufin. The homogeneity of the transfectants was assured by repeated subcloning.

Protection from B[*a*]P Toxicity in CYP1A1-expressing Normal Adherent Human Cells. The plasmid pcDNA3.1/CYP1A1 (Joshi et al., 2017) was used along with the empty plasmid pcDNA3.1 (which contained no CYP1A1 gene) for transfection (with the help of an Amaxa-Nucleofector) of adherent WI-38 cells (ATCC # CCL-75), for constructing stable cell lines. WI-38 cells were cultured in RPMI-1640 without L-glutamine (Lonza, BE12-167F) supplemented with 4 mM L-glutamine (Invitrogen, 25030024), 10% heat-inactivated fetal bovine serum (FBS; Sigma, F6178), 1% non-essential amino acids (Sigma, M7145) and 1% penicillin-streptomycin solution (Invitrogen, 15140-122).

Cells (~1 × 10^3), stably transfected with plasmid bearing a CYP gene and an empty plasmid, were seeded in a 96-well plate with different concentrations of B[*a*]P, in triplicates. Enzyme inhibition studies were carried out by co-administering the most potent inhibitors of CYP1A1 that were identified and ANF (the known CYP1A1 inhibitor) at 1 x IC_{50} concentrations, in the cell culture medium. MTT assay was performed using protocols published earlier (Mahale et al., 2014; Mahale et al., 2015). Each experiment was performed three times and statistical parameters calculated.

Reversal of Cisplatin-resistance in CYP1B1 Overexpressing Cancer Cells. This assay was performed using the protocol as reported in our earlier publications (Mohd Siddique et al., 2016; Mohd Siddique et al., 2017). The stable CYP1B1-expressing cell lines derived from PC-3 (ATCC # CRL-1435), COR-L23 (ECACC # 92031919), MIAPaca-2 ATCC (# CRL-1420) and LS174T (ATCC # CL-188), selected in the presence of G418, were maintained in RPMI-1640, supplemented with 10% fetal calf serum and 100 μg/mL normocin (Invivogen, Cat. No. ant-nr-1) at 37 ºC in a humidified incubator and maintained in a 5% CO_2 atmosphere.

Exponentially growing cells representing an asynchronous population, were trypsinised and counted in a haemocytometer using trypan blue dye exclusion method. The cells were checked for viability and then seeded in 24-well plates (Corning), at a density of 2 x 10^4 cells per well in 900 μL of complete growth medium. The plated cells were allowed to stabilize by incubating them for 24 h at 37 ºC. The CYP1B1 inhibitors were dissolved in DMSO and 10 mM stock solutions were prepared. The stock solutions of cisplatin and compounds were diluted in medium without serum. Cisplatin and 2 x IC_{50} concentration of compounds were added into the wells in triplicates while equivalent amount of DMSO was added to control wells. MTT assay was performed using earlier published protocols (Mahale et al., 2014; Mahale et al., 2015).

In Vitro Cell Proliferation Assays and Flow Cytometric Analyses. They were performed as described earlier (Mahale et al., 2014; Mahale et al., 2015). Control cells (i.e. in the absence of any compound) and cells (i.e. treated with compound) cells were harvested after treatment with trypsin. Cells were fixed in chilled (-20 ºC) 70% ethanol for an hour, after washing once with PBS. Fixed cells were centrifuged at room temperature. Pellets were re-suspended in PBS, in the presence of DNase-free ribonuclease (0.5 mg/mL; Sigma-Aldrich

R-5503) before staining with a propidium iodide solution (50 μg/mL; Sigma-Aldrich, # P-4170) for an hour (in the dark) at 4°C. Cell cycle analysis was performed on the Beckman Coulter (Epics Altra) fluorescence-activated cell sorter (Beckman Coulter UK Ltd). To exclude cell doublets or cell clumps, all events events that represent single cells were gated. Cytograms of the fluorescence peak of propidium iodide were plotted against the integrated fluorescence/linear signal. Data points on a straight line, within a single gate, were isolated and the gated data was employed for plotting a histogram that represents a complete cell cycle. The total number of events did not exceed 200 events per second. Data acquisition was stopped after collection of around 10,000 events.

Molecular modeling with CYP enzymes. The human CYP family enzymes are oxidoreductase enzymes involved in xenobiotics metabolism reactions mainly hydroxylation of aromatic and other substrates. Human P450 1B1 shares only 38% and 36% amino acid sequence identity with human P450s 1A1 and 1A2, respectively. The planner and compact structural architecture of CYP1 family members is quite different than CYP2 and CYP3 family members. The crystal structure of CYP enzymes CYP1A1 (PDB ID: 4I8V) (Walsh et al., 2013), CYP1B1 (PDB ID: 3PMO) (Wang et la., 2011), were retrieved from protein data bank and subjected to protein preparation wizard facility under default conditions implemented in Maestro v9.0 and Impact program v5.5 (Schrodinger, Inc., New York, NY, 2009). The prepared protein was further utilized to construct grid file by selecting co-crystallized ligand as centroid of grid box. For standardization of molecular docking procedure co-crystallized ligands such as ANF (CYP1A1, CYP1B1 and CYP1A2), were extracted from prepared enzyme-ligand complex and redocked to their binding site. The rest of the chemical structures were sketched, minimized and docked using GLIDE XP (Friesner et al., 2004). The ligand-protein complexes were minimized using macromodel. In order to

determine the selectivity, the corresponding binding site of CYP enzymes is flexibly aligned and analyzed with respect to CYP1A1.

Statistical Analyses. Data from experiments were analyzed by Microsoft Excel 2010 or GraphPad Prism. Student's t tests were performed to compare IC_{50} and EC_{50} values, using Excel.

Acknowledgements. The work was supported by funds from UKIERI (BC), HEIF-UK (BC) and CYP-Design Ltd (BC). MUMS acknowledge UGC-UKIERI for support of the chemistry aspect of the project and also UGC for award of MANF-JRF fellowship (201516-MANF-2015-17-MAH-60712).

REFERENCES

Aguda, B. D. 1999. A quantitative analysis of the kinetics of the G(2) DNA damage checkpoint system. Proc Natl Acad Sci U S A. 96, 11352-11357.

Androutsopoulos, V. P.; Tsatsakis, A. M.; Spandidos, D. A. 2009. Cytochrome P450 CYP1A1: wider roles in cancer progression and prevention. BMC Cancer 9, 187-203.

Basu, S.; Shaik, A. N. 2016. Is there a paradigm shift in use of microsomes and hepatocytes in drug discovery and development? ADMET & DMPK 4, 114-116.

Calabrese, E. J. 2005. Cancer biology and hormesis: human tumor cell lines commonly display hormetic (biphasic) dose responses. Crit Rev Toxicol. 35, 463-582.

Carnell, D. M.; Smith, R. E.; Daley, F. M.; Barber, P. R.; Hoskin, P. J.; Wilson, G. D.; Murray, G. I.; Everett, S. A. 2004. Target validation of cytochrome P450 CYP1B1 in

prostate carcinoma with protein expression in associated hyperplastic and premalignant tissue. Int. J. Radiat. Oncol. Biol. Phys. 58, 500-509.

Cavalieri, E. L.; Stack, D. E.; Devanesan, P. D.; Todorovic, R.; Dwivedy, I.; Higginbotham, S. M.; Johansson, S. L.; Patil, K. D.; Gross, M. L.; Gooden, J. K.; Ramanathan, R.; Cerny, R. L.; Rogan, E. G. 1997. Molecular origin of cancer: catechol estrogen-3,4-quinones as endogenous tumor initiators. Proc. Natl. Acad. Sci. USA 94, 10937-10942.

Cavalieri, E. L.; Devanesan, P.; Bosland, M. C.; Badawi, A. F.; Rogan, E. G. 2002. Catechol estrogen metabolites and conjugates in different regions of the prostate of Noble rats treated with 4-hydroxyestradiol: implications for estrogen-induced initiation of prostate cancer. Carcinogenesis 23, 329-333.

Cavalieri, E. L.; Rogan, E. G. 2004. A unifying mechanism in the initiation of cancer and other diseases by catechol quinones. Ann. N. Y. Acad. Sci. 1028, 247–257.

Chang, I.; Mitsui, Y.; Fukuhara, S.; Gill, A.; Wong, D. K.; Yamamura, S.; Shahryari, V.; Tabatabai, Z. L.; Dahiya, R.; Shin, D. M.; Tanaka, Y. 2015. Loss of miR-200c up-regulates CYP1B1 and confers docetaxel resistance in renal cell carcinoma. Oncotarget 6, 7774-7787.

Crewe, H. K.; Notley, L. M.; Wunsch, R. M.; Lennard, M. S.; Gillam, E. M. 2002. Metabolism of tamoxifen by recombinant human cytochrome P450 enzymes: formation of the 4-hydroxy, 4'-hydroxy and N-desmethyl metabolites and isomerization of trans-4-hydroxytamoxifen. Drug Metab Dispos 30, 869-874.

Daramola, O.; Stevenson, J.; Dean, G.; Hatton, D.; Pettman, G.; Holmes, W.; Field, R. 2013. A high-yielding CHO transient system: co-expression of genes encoding EBNA-1 and GS enhances transient protein expression. Biotechnol Progress 30, 132-141.

Donato, M. T.; Jimenez, N.; Castell, J. V.; Gomez-Lechon, J. M. 2004. Fluorescence-based assays for screening nine cytochrome P450 (P450) activities in intact cells expressing individual human P450 enzymes. Drug Metab Dispos. 32, 699-706.

Eastman A. 1987. The formation, isolation and characterization of DNA adducts produced by anticancer platinum complexes. Pharmacol Ther. 34, 155-166.

Fasinu, P.; Bouic, P. J.; Rosenkranz, B. 2012. Liver-based in vitro technologies for drug biotransformation Studies - A Review. Curr. Drug. Metab. 13, 215-224.

Flied, L.; Grillari, J.; Grillari-Voglauer, R. 2015. Human cell lines for the production of recombinant proteins: on the horizon. N Biotechnol. 32, 673–679.

Friesner, R. A.; Banks, J. L.; Murphy, R. B.; Halgren, T. A.; Klicic, J. J.; Mainz, D. T.; Repasky, M. P.; Knoll, E. H.; Shelley, M.; Perry, J. K.; Shaw, D. E.; Francis, P.; Shenkin, P. S. 2004. Glide: A New Approach for Rapid, Accurate Docking and Scoring. 1. Method and Assessment of Docking Accuracy. J. Med. Chem. 47, 1739–1749.

Gajjar, K.; Martin-Hirsch, P. L.; Martin, F. L. 2012. CYP1B1 and hormone-induced cancer. Cancer Lett. 324, 13–30.

Han, X.; Sunc, L.; Fang, Q.; Li, D.; Gong, X.; Wu, Y.; Yang, S. Y.; Shen, B. Q. 2007. Transient expression of osteopontin in HEK 293 cells in serum-free culture. Enz Micro Tech. 41, 133-140.

Hausjell, J.; Halbwirth, H.; Spadiut, O. 2018. Recombinant Production of Eukaryotic Cytochrome P450s in microbial cell factories. Biosci Rep. doi: 10.1042/BSR20171290. [Epub ahead of print].

Hayes, C. L.; Spink, D. C.; Spink, B. C.; Cao, J. Q.; Walker, N. J.; Sutter, T. R. 1996. 17b-estradiol hydroxylation catalyzed by human cytochrome P450 1B1. Proc. Natl. Acad. Sci. USA 93, 9776-9781.

Horley, N. J.; Beresford, K. J.; Chawla, T.; McCann, G. J.; Ruparelia, K. C.; Gatchie, L.; Sonawane, V. R.; Williams, I. S.; Tan, H. L.; Joshi, P.; Bharate, S. S.; Kumar, V.; Bharate, S. B.; Chaudhuri, B. 2017. Discovery and characterization of novel CYP1B1 inhibitors based on heterocyclic chalcones: Overcoming cisplatin resistance in CYP1B1-overexpressing lines. Eur J Med Chem 129, 159-174.

Joshi, P.; McCann, G. J. P.; Sonawane, V. R.; Vishwakarma, R. A.; Chaudhuri, B.; Bharate, S. B. 2017. Identification of potent and selective CYP1A1 inhibitors via combined ligand and structure-based virtual screening and their in vitro validation in Sacchrosomes and live human Cells. J Chem Inf Model 57, 1309-1320.

Lao, X.; Qin, X.; Peng, Q.; Chen, Z.; Lu, Y.; Liu, Y.; Li, S. 2014. Association of CYP1B1 Leu432Val polymorphism and lung cancer risk: an updated meta-analysis. Lung 192, 739-48.

Lewis, D. F. 2004. 57 varieties: the human cytochromes P450. Pharmacogenomics 5, 305-318.

Li, C.; Long, B.; Qin, X.; Li, W.; Zhou, Y. 2015. Cytochrome P1B1 (CYP1B1) polymorphisms and cancer risk: a meta-analysis of 52 studies. Toxicology 327, 77-86.

Liehr, J. G.; Ricci, M. J. 1996. 4-Hydroxylation of estrogens as marker of human mammary tumors. Proc. Natl. Acad. Sci. USA 93, 3294-3296.

Macallister R,; Scholield C,; Petmann G,; Mannix G.; 1999. Adaptation of recombinant HEK293 to growth in serum free suspension. In Animal Cell Technology: Products from cell, cells as product. Bernard, A., Griffiths, B., Noe, W., Wurm, F editors, Kluwer Academic Publisher, Netherlands: Springer. 367-369.

Mahmood, T.; Yang, P. C. 2012. Western Blot: Technique, Theory, and Trouble Shooting. N Am J Med Sci. 4, 429–434.

Martinez, V. G.; O'Connor, R.; Liang, Y.; Clynes, M. 2008. CYP1B1 expression is induced by docetaxel: effect on cell viability and drug resistance. Br. J. Cancer 98, 564–570.

Mahale, S.; Bharate, S. B.; Manda, S.; Joshi, P.; Bharate, S. S.; Jenkins, P. R.; Vishwakarma, R. A.; Chaudhuri, B. 2014. Biphenyl-4-carboxylic acid [2-(1H-indol-3-yl)-ethyl]-methylamide (CA224), a nonplanar analogue of fascaplysin, inhibits Cdk4 and tubulin polymerization: evaluation of in vitro and in vivo anticancer activity. J. Med. Chem. 57, 9658–9672.

Mahale, S.; Bharate, S. B.; Manda, S.; Joshi, P.; Jenkins, P. R.; Vishwakarma, R. A.; Chaudhuri, B. 2015. Antitumour potential of BPT: a dual inhibitor of cdk4 and tubulin polymerization. Cell Death Dis. 6, e1743.

Mazur, C. S.; Kenneke, J. F.; Goldsmith, M. R.; Brown, C. 2009. Contrasting influence of NADPH and a NADPH-regenerating system on the metabolism of carbonyl-containing compounds in hepatic microsomes. Drug Metab Dispos. 37, 1801-1805.

McFadyen, M. C.; Breeman, S.; Payne, S.; Stirk, C.; Miller, I. D.; Melvin, W. T.; Murray, G. I. 1999. Immunohistochemical localization of cytochrome P450 CYP1B1 in breast cancer with monoclonal antibodies specific for CYP1B1. J. Histochem. Cytochem. 47, 1457-1464.

Mei, Q.; Zhou, D.; Han, J.; Lu, H.; Tang, B. 2012. CYP1B1 Asn453Ser polymorphism and colorectal cancer risk: a meta-analysis. Metabolism 61, 1321-1329.

Meissner, P.; Pick, H.; Kulangara, A.; Chatellard, P.; Friedrich, K.; Wurm, F. M. 2001. Transient gene expression: recombinant protein production with suspension-adapted HEK293-EBNA cells. Biotechnol and Bioeng 75, 197-203.

Moorthy, B.; Chu, C.; Carlin, D. J. 2015. Polycyclic aromatic hydrocarbons: from metabolism to lung cancer. Toxicol Sci. 145, 5-15.

Mohd Siddique, M. U.; McCann, G. J. P.; Sonawane, V. R.; Horley, N.; Gatchie, L.; Joshi, P.; Bharate, S. B.; Jayaprakash, V.; Sinha, B. N.; Chaudhuri, B. 2017. Quinazoline derivatives as selective CYP1B1 inhibitors. Eur. J. Med. Chem. 130, 320-327.

Mohd Siddique, M. U.; McCann, G. J.; Sonawane, V.; Horley, N.; Williams, I. S.; Joshi, P.; Bharate, S. B.; Jayaprakash, V.; Sinha, B. N.; Chaudhuri, B. 2016. Biphenyl urea derivatives as selective CYP1B1 inhibitors. Org. Biomol. Chem. 14, 8931-8936.

Murray, G. I.; Taylor, M. C.; McFadyen, M. C.; McKay, J. A.; Greenlee, W. F.; Burke, M. D.; Melvin, W. T. 1997. Tumor-specific expression of cytochrome P450 CYP1B1. Cancer Res. 57, 3026-3031.

Muskhelishvili, L.; Thompson, P. A.; Kusewitt, D. F.; Wang, C.; Kadlubar, F. F. 2001, In situ hybridization and immunohistochemical analysis of cytochrome P450 1B1 expression in human normal tissues. J Histochem Cytochem 49, 229–236.

Nebert, D.W.; Wikvall, K.; Miller, W.L. 2013. Human cytochromes P450 in health and disease. Philosoph. Trans. Royal Soc. B: Biol. Sci. 368, 20120431.

Nebert, D. W.; Russell, D. W. Clinical importance of the cytochromes P450. 2002. Lancet 360, 1155–1162.

Newbold, R. R.; Liehr, J. G. 2000. Induction of uterine adenocarcinoma in CD-1 mice by catechol estrogens. Cancer Res. 60, 235 -237.

Rogan, E. G.; Badawi, A. F.; Devanesan, P. D.; Meza, J. L.; Edney, J. A.; West, W. W.; Higginbotham, S. M.; Cavalieri, E. L. 2003. Relative imbalances in estrogen metabolism and conjugation in breast tissue of women with carcinoma: potential biomarkers of susceptibility to cancer. Carcinogenesis 24, 697-702.

Rochat, B.; Morsman, J. M.; Murray, G. I.; Figg, W. D.; McLeod, H. L. 2001. Human CYP1B1 and anticancer agent metabolism: mechanism for tumor-specific drug inactivation? J. Pharmacol. Exp. Ther. 296, 537–541.

Schiering, C.; Wincent, E.; Metidji, A.; Iseppon, A.; Li, Y.; Potocnik, A. J.; Omenetti, S.; Henderson, C. J.; Wolf, C. R.; Nebert, D. W.; Stockinger, B. 2017. Feedback control of AHR signalling regulates intestinal immunity. Nature 542, 242-245.

Spink, D. C.; Spink, B. C.; Cao, J. Q.; De Pasqualle, J. A.; Pentecost, B. T.; Fasco, M. J.; Li, Y.; Sutter, T. R. 1998. Differential expression of CYP1A1 and CYP1B1 in human breast epithelial cells and breast tumor cells. Carcinogenesis 19, 291-298.

Sutter, T. R.; Tang, Y. M.; Hayes, C. L.; Wo, Y. Y. P.; Jabd, E. W.; Li, X.; Yin, H.; Cody, C. W.; Greenlee, W. F. 1994. Complete cDNA sequence of a human dioxin-inducible mRNA identifies a new gene subfamily of cytochrome P450 that maps to chromosome 2. J. Biol. Chem. 269, 13092-13099.

Tait, L.; Soule, H. D.; Russo, J. 1990. Ultrastructural and immunocytochemical characterization of an immortalized human breast epithelial cell line, MCF-10. Cancer Res. 50, 6087-6094.

Vrana D, Novotny J, Holcatova I, Hlavata I, Soucek P. 2010. CYP1B1 gene polymorphism modifies pancreatic cancer risk but not survival. Neoplasma 57, 15-19.

Walsh, A. A.; Szklarz, G. D.; Scott, E. E. 2013. Human Cytochrome P450 1A1 Structure and Utility in Understanding Drug and Xenobiotic Metabolism. J. Biol. Chem. 288, 12932–12943.

Wang, A.; Savas, U.; Stout, C. D.; Johnson, E. F. 2011. Structural characterization of the complex between α-naphthoflavone and human cytochrome CYP1B1. J. Biol. Chem. 286, 5736–5743.

Yager, J. D. 2000. Endogenous estrogens as carcinogens through metabolic activation. J. Natl. Cancer Inst. Monographs, 27, 67-73.

Zhu, B. T.; Conney, A. H. 1998. Functional role of estrogen metabolism in target cells: review and perspectives. Carcinogenesis 19, 1-27.

FIGURE LEGENDS

Scheme 1. Synthesis of quinazolinones **5a-i**, **7a-g** and **9a-k**. Reagents and conditions: (a) K_2CO_3, KI, acetone, reflux, 8-10 h. (b) I_2, sodium acetate, DMF, 60-70 °C, 24 h.

Figure 1. Adaptation of HEK293 monolayer adherent cells to serum-free 'suspension' culture to obtain HEK293S cells. **(A)** Photomicrograph (20x magnification) of HEK293 adherent cells grown as a monolayer culture on T75 mm^3 flask in EMEM medium supplemented with 10% FBS, using an Olympus BX-51 fluorescence microscope. **(B)** Photomicrograph (20x) of HEK293S cells, after adaptation to serum-free 'suspension' culture, grown in 125 mL Erlenmeyer polycarbonate EML flasks. **(C)** Photomicrograph (10x) of HEK293S cells, adapted to serum-free ''suspension'' culture in 125 mL EML flask, co-transfected with plasmids encoding eGFP and CYP1A1, 24 h post-transfection. **(D)** Fluoroscopic photomicrograph (10x) of the same cells as in (1C). **(E)** Overlay of photomicrographic images (C) and (D), depicting population of cells with eGFP expression; in theory, these HEK293S cells should also contain the CYP1A1 plasmid.

Figure 2. Activity of CYP1A1 enzyme in live HEK293S cells, transfected with the plasmid pCDL/CYP1A1 (Figure S1), and inhibition of the cellular enzyme by α-naphthoflavone (ANF). **(A)** Expression of CYP1A1, in 5 µg of total protein, isolated from HEK293S cells, was confirmed by Western blotting (middle lane). Left-hand lane depicts HEK293S cells (5 µg of total protein), carrying the empty plasmid pCDL, which show no expression. CYP1A1-bearing Sacchrosomes™ (3 pmol) were taken as positive control (right-hand lane). The house-keeping protein, β-actin, served as a loading control. **(B)** 24 h post-transfection, HEK293S cells (100 x 10^3) were seeded in triplicates in 96-well black plates and CYP1A1 enzyme activity was determined by adding 5 µM 7-ER (7-ethoxy-resorufin) and the formation of resorufin as fluorescent product was measured at excitation-560 nm/emission-590 nm on a Biotek Synergy HT plate reader. The wells of the plate were read over a period of 1 h and net RFUs (relative fluorescence units) were considered for representing the graphs. **(C)** Activity of CYP1A1 enzyme, within HEK293S cells, was measured (n=3) at 24, 48, 72, 96 and 120 h post-transfection. **(D)** 24 h post-transfection, live cell inhibition assay (n=3) for

CYP1A1 enzyme. HEK293S (100 x 10^3) cells, expressing CYP1A1 enzyme, were seeded in triplicates in 96-well black plate. ANF (in different concentrations) was added to wells and incubated for 30 min at 37 ºC, 8% CO_2, with 7-ER as substrate. The IC_{50} value for inhibition of CYP1A1 (0.383 µM ± 0.05) is mean of three independent experiments.

Figure 3. Activity of CYP1B1 enzyme in live HEK293S cells transfected with the plasmid pCDL/CYP1B1 (Figure S2) and inhibition of the cellular enzyme by ANF. **(A)** Expression of CYP1B1, in HEK293S cells (5 µg of total protein), was confirmed by Western blotting (middle lane). Left-hand lane depicts HEK293S cells (5 µg of total protein), carrying the empty plasmid pCDL, which shows no expression. CYP1B1-bearing Sacchrosomes™ (2 pmol) were taken as positive control (right-hand lane). The β-actin protein served as a loading control. **(B)** 24 h post-transfection, the activity of CYP1B1 enzyme, within HEK293S cells, were measured (n=3). 200 x 10^3 HEK293S cells, expressing CYP1B1 enzyme, were seeded in triplicates in 96-well black plates. Formation of fluorescent product, resorufin, was measured over a period of an hour, in kinetic mode, on a Biotek Synergy HT plate reader after addition of 5 µM fluorogenic substrate, 7-ER. Net RFUs were considered for representing the graphs. **(C)** CYP1B1 enzyme activity in HEK293S cells were measured (n=3) at 24, 48, 72, 96 and 120 h post-transfection, using 7-ER as a substrate. **(D)** Inhibition (n=3) of CYP1B1 enzyme within live HEK293S cells. 200 x 10^3 cells, expressing CYP1B1 enzyme, along with the CYP1B1 inhibitor, ANF, in varying concentrations, were added to wells and incubated for 30 min at 37 ºC, 8% CO_2. The IC_{50} value for inhibition of CYP1B1 (0.052 µM ± 0.01) is mean ± SE of three independent experiments.

Figure 4. Molecular modeling studies. (A) Interactions of **7b** with CYP1B1. (B) Interactions of **9b** with CYP1B1. (C) Overlay of **7b** and **9b** with CYP1B1.

Figure 5. FACS analyses of stable transfectants of WI-38 cells, bearing the plasmid pcDNA3.1/CYP1A1 and treated with B[*a*]P, in the absence of a CYP1A1 inhibitor (B) and in the presence of the CYP1A1-specific inhibitors, compound **7g** (C), compound **9i** (D). (A) Shows untreated 'control' cells growing asynchronously. Cells were transfected with the plasmid pcDNA3.1/CYP1A1[36] and pcDNA3.1 using Amaxa-Nucleofector. Stable clones

were selected using the antibiotic G418. The ratio of the percentage of cells in G_0/G_1 and S phases of the cell division cycle is shown in the upper right-hand corner of each of the FACS analyses. (E) Western blot confirming the expression of CYP1A1 in WI-38::pcDNA3.1/CYP1A1 cells. Lane 1, Expression of CYP1A1, in WI-38 cells transfected with the plasmid pcDNA3.1/CYP1A1 (5 μg of total protein). Lane 2, WI-38 cells, transfected with the empty plasmid, pcDNA3.1 (5 μg of total protein), which show no expression. Lane 3, CYP1A1-bearing Sacchrosomes™ (3 pmol) were taken as positive control. The β-actin protein (lower panel) served as a loading control.

Figure 6. Expression of CYP1B1, in different cancer cell lines, as monitored via Western blotting. Lane 1, 5 μg of total protein from cells stably transfected with the plasmid, pcDNA3.1/CYP1B1; lane 2, 5 μg of total protein from cells stably transfected with the empty plasmid pcDNA3.1; lane 3, CYP1B1-bearing Sacchrosomes™ (2 pmol) were taken as positive control. The β-actin protein served as a loading control (lower panels of (A) to (D)). Proteins from (A) PC-3 (prostate cancer) cells; (B) COR-L23 (lung cancer) cells; (C) MIAPaca-2 (pancreatic cancer) cells; and (D) LS174T (colon cancer) cells.

Figure 7. Determination of EC_{50} values for cisplatin in the absence or presence of the CYP1B1 inhibitor, compound **9b**, in four different cancer cell lines, PC-3, COR-L23, MIAPaca-2 and LS174T that express CYP1B1. The values presented for IC_{50} determinations represent mean ± S.D. of three independent experiments ($^*P < 0.1$; one-tailed Student's t-test). Graphs show that there is a dramatic decrease of cisplatin's EC_{50} values when cells are pre-incubated with the CYP1B1-specific inhibitor, compound **9b**. The results obtained from these graphs have also been presented in Table 9.

Figure 8. FACS analyses showing the four CYP1B1-specific inhibitors (compounds **5e**, **7b**, **7c** and **9b**) re-sensitize CYP1B1-overexpressing MIAPaCa-2::pcDNA3.1/CYP1B1 pancreatic cells (i.e. MIAPaCa-1B1) to cisplatin's toxicity. (A) MIAPaCa-1B1 cells treated with an EC_{50} concentration (70 μM) of cisplatin (CP). (B) to (E), MIAPaCa-1B1 cells pre-treated with 2x IC_{50} concentration of compound (cpd). followed by treatment with EC_{50}

concentration of cisplatin, 3.9, 3.7, 3.7, or 3.5 µM, depending on the inhibitory compound used (see Table 9).

Figure 9. FACS analyses shows that pre-incubation with compound **9b** (2x IC_{50} concentration) of (A) PC-3-1B1, (B) COR-L23-1B1, (C) LS174T-1B1 cells, which stably express human CYP1B1 enzyme, re-sensitizes the recombinant cells to cisplatin's (CP's) toxic effects at its EC_{50} concentrations in these cells (2.7 µM for PC-3-1B1; 3.6 µM for COR-L23-1B1; and 3.4 µM for LS174T-1B1; see Table 9).

TABLES

Table.1. IC_{50} values of CYP-specific inhibitors. Comparison of inhibition of CYP enzymes expressed within human HEK293S cells with those present in hepatocytes, HLMs (human liver microsomes) and recombinant CYP-bearing microsomes (Sacchrosomes, Supersomes and Bactosomes). 'NF' designates 'not found' in the literature.

CYP enzymes		IC_{50} (µM)					
		Live cell assays		**Microsomal assays**			
		Hepatocytes (Literature)	CYP-expressing HEK293S cells	HLM (Literature)	Sacchrosomes	Supersomes (Literature)	Bactosomes (Literature)
Source	Inhibitor	Human	Human (this	Human	Yeast #	Insect	Bacteria
1A1	ANF	0.1-0.46 [41]	0.383	0.19 [42]	0.01	0.018 [43]	NF
1A2	ANF	0.096 [44]	0.078	0.016 [42]-0.26 [45]	0.03	0.0081-0.28 [46]	0.0032 [47]
	Furafylline	2.92 [48]	3.4	0.6 - 0.73 [44], 5.26 [49]	2–3.9	5.22 [46], 6 [50]	43.2-62.95 [51]
1B1	ANF	NF	0.052	0.03 [42]	0.05	NF	0.034 #
2D6	Quinidine	0.03-0.1 [48]	0.0172	0.13 [52], 0.02 [53], 0.47 [54]	0.0045	0.002 - 0.22 [50]	0.048 [47]
2C9	Sulfaphenazole	0.1- 0.46 [48]	0.105	0.194 [47] - 0.51 [42]	1.1	0.11 -1.23 [46,50]	0.21 [51] -1.2 [47]
2C19	Ticlopidine	0.1 [48]	0.0688	0.23 [42]	3.5	0.04 [46] - 2.7 [55]	0.52 [51]
3A4	Ketoconazole	0.114 [48] - 0.3 [41]	0.0034	0.0037 - 0.18 [44]	0.27	0.165 [47]	0.21, 0.065 [47]

Table 2. Percentage inhibition of CYP1A1 and CYP1B1 by quinazolinones **5a-i** in Sacchrosomes™, Bactosomes™, Supersomes™ and in live human HEK293S cells.

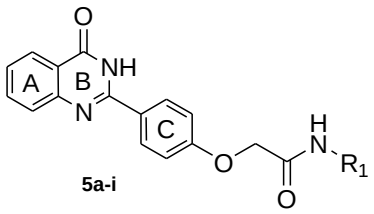

5a-i

Entry	R_1	IC_{50} (μM) for **CYP1A1** inhibition				IC_{50} (μM) for **CYP1B1** inhibition			
		Sacchrosomes	Bactosomes	Supersomes	'live' human HEK293S cells	Sacchrosomes	Bactosomes	Supersomes	'live' human HEK293S cells
5a	cyclohexyl	>20	>20	>20	>20	>10	>10	>10	>50
5b	-Ph	>10	>10	>10	>20	>10	>10	>10	>50
5c	p-tolyl	4.8 ± 0.3	5.6 ± 0.2	4.9 ± 0.4	>20	>10	>10	>10	>50
5d	-Ph(3-Cl)	4.5 ± 0.2	5.2 ± 0.5	4.8 ± 0.4	>20	7.4 ± 0.4	7.1 ± 0.5	8.2 ± 0.8	8.9 ± 0.2
5e	-Ph(4-NO_2)	6.1 ± 0.1	6.9 ± 0.6	6.4 ± 0.4	>20	4.1 ± 0.2	4.5 ± 0.3	5.1 ± 0.5	0.042 ± 0.002
5f	-Ph(4-OEt)	>50	>20	>20	>10	>10	>10	>10	>10
5g	2-naphthyl	>20	>20	>20	2.8 ± 0.1	>10	>10	>10	1.0 ± 0.04
5h	1-naphthyl	>20	>20	>20	9.1 ± 0.2	>10	>10	>10	6.7 ± 0.2
5i	phenylethyl	>20	>20	>20	>20	>50	>50	>10	>10

All values, presented in μM concentrations, represent the mean and standard deviations of three independent experiments ($^{*}P < 0.1$; one-tailed Student's t-test).

Table 3. Percentage inhibition of CYP1A1 and CYP1B1 by quinazolinones **7a-g** in Sacchrosomes™, Bactosomes™, Supersomes™ and in live human HEK293S cells.

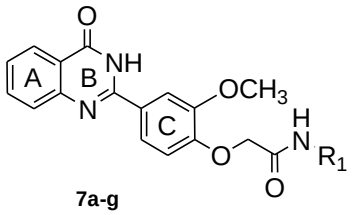

7a-g

Entry	R_1	IC_{50} (µM) for **CYP1A1** inhibition				IC_{50} (µM) for **CYP1B1** inhibition			
		Sacchrosomes	Bactosomes	Supersomes	'live' human HEK293S cells	Sacchrosomes	Bactosomes	Supersomes	'live' human HEK293S cells
7a	**n-butyl**	9.9 ± 0.4	>10	>10	>20	10.2 ± 0.3	10.7 ± 0.5	>10	7.5 ±0.3
7b	**-Ph(2-OMe)**	>50	>20	>20	>10	5.8 ± 0.1	5.4 ± 0.3	6.9 ±0.7	0.032 ± 0.002
7c	**-Ph(3-OMe)**	3.5 ± 0.2	4.8 ± 0.4	3.7 ± 0.3	2.1 ± 0.2	0.085 ± 0.003	0.093 ± 0.008	0.152 ±0.015	0.039 ± 0.002
7d	**-Ph(4-OMe)**	6.8 ± 0.3	7.6 ± 0.3	6.9 ± 0.3	8.9 ± 0.1	8.8 ± 0.2	8.4 ± 0.4	9.8 ± 0.2	8.9 ± 0.02
7e	**-Ph(4-OEt)**	9.7 ± 0.4	>10	>10	1.7 ± 0.1	5.5 ± 0.2	5.1 ± 0.5	6.8 ± 0.4	5.9 ± 0.1
7f	**-Ph(4-F)**	>20	>20	>20	>10	0.9 ± 0.03	0.8 ± 0.06	2.1 ± 0.05	0.8 ± 0.02
7g	**2-Naphthyl**	4.7 ± 0.1	5.7 ± 0.4	5.2 ± 0.3	0.06 ± 0.002	6.5 ± 0.2	6.7 ± 0.3	7.8 ± 0.6	4.6 ± 0.1

All values, presented in µM concentrations, represent the mean and standard deviations of three independent experiments ($^{*}P < 0.1$; one-tailed Student's t-test).

Table 4. Percentage inhibition of CYP1A1 and CYP1B1 by quinazolinones **9a-k** in Sacchrosomes™, Bactosomes™, Supersomes™ and in live human HEK293S cells.

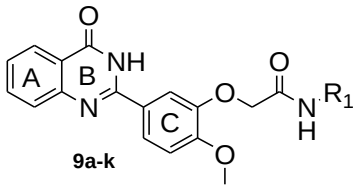

9a-k

Entry	R_1	IC_{50} (μM) for **CYP1A1** inhibition				IC_{50} (μM) for **CYP1B1** inhibition			
		Sacchrosomes	Bactosomes	Supersomes	'live' human HEK293S cells	Sacchrosomes	Bactosomes	Supersomes	'live' human HEK293S cells
9a	-Ph	3.0 ±0.1	3.8 ± 0.2	3.2 ± 0.2	9.4 ± 0.2	5.4 ± 0.2	5.8 ± 0.4	5.4 ±0.2	0.7 ± 0.02
9b	-Ph(2-OMe)	>20	>20	>20	2.3 ± 0.1	1.3 ± 0.1	1.6 ± 0.1	1.7 ± 0.2	0.021 ± 0.001
9c	-Ph(3-OMe)	7.8 ± 0.3	8.8 ± 0.5	8.2 ±0.3	0.35 ± 0.08	2.2 ± 0.1	2.7 ± 0.3	2.4 ± 0.1	9.2 ± 0.2
9d	-Ph(4-OMe)	5.2 ±0.1	6.7 ±0.1	5.8 ±0.1	>20	>10	>10	>10	9.1 ± 0.2
9e	-Ph(4-OEt)	>20	>20	>20	>20	>10	>10	>10	>10
9f	-Ph(2-Me)	7.9 ± 0.2	9.1 ± 0.7	8.2 ±0.2	>10	>10	>10	>10	8.9 ± 0.2
9g	-Ph(2-Cl)	>20	>20	>20	>20	>10	>10	>10	>10
9h	-Ph(4-Cl)	6.6 ± 0.4	7.7 ± 0.5	7.2 ± 0.4	8.3 ± 0.5	9.1 ±0.2	9.9 ± 0.6	9.4 ± 0.4	9.3 ± 0.5
9i	-Ph(4-F)	>10	>10	>10	0.03 ± 0.001	>10	>10	>10	7.8 ± 0.3

9j	-Ph(4-NO_2)	>20	>20	>20	>20	>10	>10	>10	>10
9k	n-butyl	>20	>20	>20	>10	>10	>10	>10	>10

All values, presented in μM concentrations, represent the mean and standard deviations of three independent experiments ($^{*}P < 0.1$; one-tailed Student's t-test).

Table 5. Specificity of the potent CYP1A1 and CYP1B1 inhibitors, identified in HEK293S-cell-assays, with respect to inhibition of other CYPs expressed within HEK293S cells.

Entry	IC_{50} (μM)						
	1A1	1B1	1A2	2C9	2C19	2D6	3A4
5e	>20	0.042 ± 0.002	>20	>10	>10	>10	>10
5g	2.8 ±0.1	1.0 ± 0.04	9.8 ± 0.07	>10	>10	>10	>10
7b	10.8±0.3	0.032 ± 0.002	11.1 ± 0.1	>10	>10	>10	>10
7c	2.1 ±0.2	0.039 ± 0.002	8.5 ± 0.07	>10	>10	>10	>10
7e	1.7 ± 0.1	5.9 ± 0.1	>10	>10	>10	>10	>10
7f	12 ±0.5	0.8 ± 0.02	>10	>10	>10	>10	>10
7g	0.06 ±0.002	4.6 ± 0.1	7.8 ± 0.07	>10	>10	>10	>10
9a	9.4 ±0.2	0.7 ± 0.02	12.8 ± 0.1	>10	>10	>10	>10
9b	2.3 ±0.1	0.021 ± 0.001	>10	>10	>10	>10	>10
9c	0.35 ±0.08	9.2 ± 0.2	>10	>10	>10	>10	>10
9i	0.03 ± 0.001	7.8 ± 0.3	>10	>10	>10	>10	>10

All values, presented in μM concentrations, represent the mean and standard deviations of three independent experiments.

Table 6. EC_{50} values of B[*a*]P after treatment of cells with a range of concentrations of B[*a*]P (0.05 µM- 100 µM) [a].

Cell Line	EC_{50} of B[*a*]P (µM)
WI-38:: –	18 ± 0.8
WI-38:: pcDNA3.1	17.2 ± 0.9
WI-38:: pcDNA3.1/hCYP1A1	0.8 ± 0.2

[a] The cells used were: (a) untransfected WI-38 cells (WI-38:: –), (b) WI-38::pcDNA3.1 cells (WI-38 cells transfected with pcDNA3.1, a basic plasmid which does not contain a gene insert) and (c) WI-38::pcDNA3.1/hCYP1A1 cells (WI-38 cells transfected with the plasmid pcDNA3.1/hCYP1A1[36] which encodes the human CYP1A1 gene). Transfection of plasmids was conducted with the help of Amaxa-Nucleofector, following instructions provided by Amaxa. Stable clones were selected using G418 (neomycin); pcDNA3.1 encodes the neomycin resistance gene. A range of concentrations of B[*a*]P (0.05 µM – 100 µM) were used to determine the EC_{50} values via the MTT assay. All values, presented in µM concentrations, represent the mean and standard deviations of three independent experiments ($^{*}P < 0.1$; one-tailed Student's t-test).

Table 7. EC_{50} values (in μM) of B[*a*]P after pre-treatment of WI-38::pcDNA3.1/hCYP1A1 cells with an IC_{50} concentration of a CYP1A1 inhibitor, followed by treatment of cells with a range of concentrations of B[*a*]P [a].

Entry	CYP1A1, IC_{50}, in human cells	EC_{50}, compound + B[*a*]P (EC_{50}, B[*a*]P alone)
7c	2.1	6.2 ± 0.2 (0.8)
7e	1.7	7.8 ± 0.4 (0.8)
7g	0.06	16.9 ± 0.6 (0.8)
9c	0.35	14.8 ± 0.4 (0.8)
9i	0.03	17.0 ± 0.6 (0.8)
ANF	>10	1.9 ± 0.3 (0.8)

[a] A range of concentrations of B[*a*]P (0.05 μM – 100 μM) were used, in the presence of 1x IC_{50} values of compounds (as was determined in the HEK293S-cell-assay), whereas ANF (α-naphthoflavone) was used at 20 μM concentration. All values, presented in μM concentrations, represent the mean and standard deviations of three independent experiments ($^{*}P < 0.1$; one-tailed Student's t-test). The recombinant WI-38::pcDNA3.1/hCYP1A1 stable cell line was tested for ethoxyresorufin-O-deethylase (EROD) activity, using7-ethoxyresorufin as a substrate. CYP1A1 expression in these cells was confirmed by Western blotting (Figure 5E).

Table 8. EC_{50} values of cisplatin after treatment of (a) untransfected cancer cells, and (b)/(c) in the absence/presence of a plasmid bearing the human CYP1B1 gene, with a range of concentrations of cisplatin (0 µM – 500 µM) [a].

Cell line	Cell lines with transfection	EC_{50}values of cisplatin (µM)
PC-3	(a) PC-3:: –	3.5 ± 0.4
	(b) PC-3::pcDNA3.1	3.0 ± 0.3
	(c) PC-3::pcDNA3.1/CYP1B1	50.0 ± 7
COR-L23	(a) COR-L23:: –	4.5 ± 0.6
	(b) COR-L23::pcDNA3.1	3.9 ± 0.6
	(c) COR-L23::pcDNA3.1/CYP1B1	63.0 ± 7
MIAPaCa-2	(a) MIA PaCa-2:: –	4.2 ± 0.6
	(b) MIA PaCa-2::pcDNA3.1	3.8 ± 0.5
	(c) MIA PaCa-2::pcDNA3.1/CYP1B1	70.0 ± 4
LS174T	(a) LS174T:: –	4.3 ± 0.3
	(b) LS174T::pcDNA3.1	3.7 ± 0.4
	(c) LS174T::pcDNA3.1/CYP1B1	90.0 ± 7

[a] The cells used were: (a) untransfected cells (PC-3/COR-L23/MIAPaca-2/LS174T:: –), (b) PC-3/COR-L23/MIAPaca-2/LS174T:: pcDNA3.1 cells transfected with pcDNA3.1 (i.e. the basic plasmid which does not contain a gene insert) and (c) PC-3/COR-L23/MIAPaca-2/LS174T:: pcDNA3.1/hCYP1B1 cells transfected with pcDNA3.1/hCYP1B1[33] (i.e. the plasmid which encodes the human CYP1B1 gene). Cells were transfected with the help of Amaxa-Nucleofector. Stable clones were selected using G418 (neomycin); the plasmid, pcDNA3.1, encodes the neomycin resistance gene. A range of concentrations of cisplatin (0 µM – 500 µM) were used to determine the EC_{50} values via the MTT assay. All values, presented in µM concentrations, represent the mean and standard deviations of three independent experiments ($^{*}P < 0.1$; one-tailed Student's t-test).

Table 9. EC_{50} values (in μM) of cisplatin (CP), after pre-incubating stable CYP1B1-expressing human cancer cells, PC-3/COR-L23/MIAPaca-2/LS174T, with a CYP1B1 inhibitor [2x IC_{50}], followed by treatment with different concentrations of cisplatin [a].

Compound Name	CYP1B1, IC_{50}, in human cells	EC_{50}, PC-3 (EC_{50}, CP alone)	EC_{50}, COR-L23 (EC_{50}, CP alone)	EC_{50}, MIAPaCa-2 (EC_{50}, CP alone)	EC_{50}, LS174T (EC_{50}, CP alone)
5e	0.042	3.1 ± 0.3 (50)	4.0 ± 0.3 (63)	3.9 ± 0.3 (70)	3.6 ± 0.3 (90)
7b	0.032	2.9 ± 0.2 (50)	3.8 ± 0.3 (63)	3.7 ± 0.3 (70)	3.5 ± 0.2 (90)
7c	0.039	3.0 ± 0.3 (50)	4.0 ± 0.5 (63)	3.7 ± 0.3 (70)	3.5 ± 0.2 (90)
7d	0.9	3.7 ± 0.3 (50)	4.3 ± 04 (63)	4.0 ± 0.3 (70)	3.9 ± 0.3 (90)
7e	1.9	4.5 ± 0.6 (50)	4.6 ± 0.6 (63)	4.3 ± 0.3 (70)	4.2 ± 0.3 (90)
5a	>10	54.3 ± 3 (50)	65.2 ± 6 (63)	73.2 ± 8 (70)	93.0 ± 8 (90)
9a	0.7	3.7 ± 0.3 (50)	4.3 ± 0.5 (63)	4.0 ± 0.3 (70)	3.8 ± 0.3 (90)
9b	0.021	2.7 ± 0.1 (50)	3.6 ± 0.3 (63)	3.5 ± 0.3 (70)	3.4 ± 0.3 (90)
9h	1.3	4.2 ± 0.6 (50)	4.5 ± 0.6 (63)	4.2 ± 0.3 (70)	4.2 ± 0.3 (90)
9e	>10	56.5 ± 6 (50)	67.5 ± 6 (63)	76.5 ± 6 (70)	92.5 ± 6 (90)
ANF	>5	46.5 ± 4 (50)	57.5 ± 3 (63)	67.5 ± 6 (70)	87.5 ± 7 (90)

[a] A range of concentrations of cisplatin (0 μM – 500 μM) were used, in the presence of 2x IC_{50} values of compounds (as was determined in the live HEK293S-cell-assay, where cells were grown in 'suspension'), whereas ANF was used at 20 μM concentration. All values, presented in μM concentrations, represent the mean and standard deviations of three independent experiments ($^{*}P < 0.1$; one-tailed Student's t-test). All cell lines were tested for expression of CYP1B1, an ethoxyresorufin-O-deethylase (EROD), using7-ethoxyresorufin as a substrate. CYP1B1 expression, in all four cancer cell lines, was also confirmed using Western blotting (Figure 6).

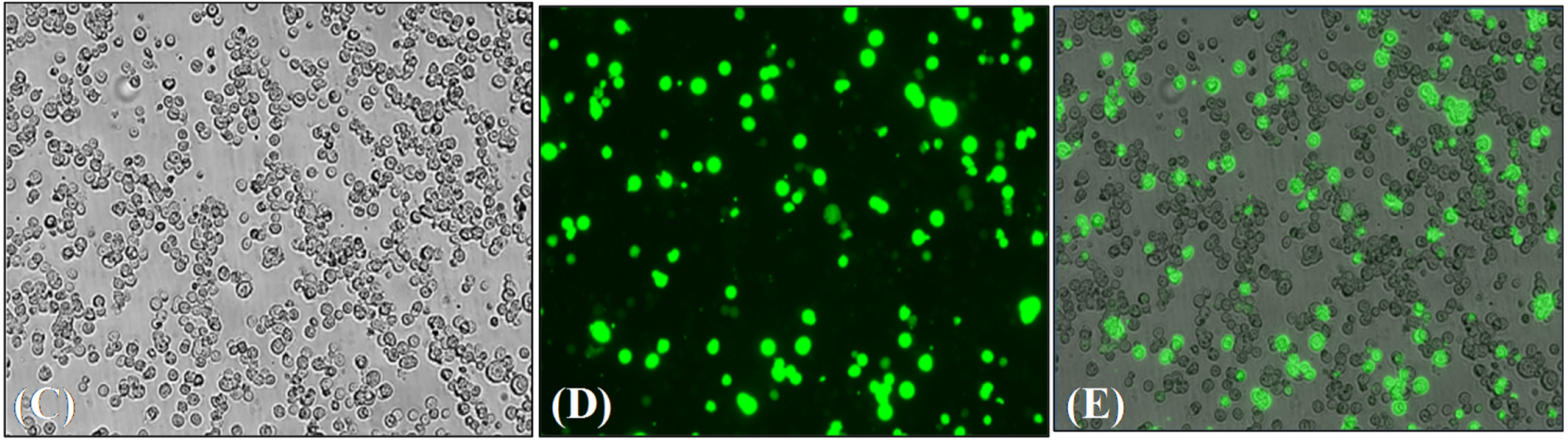

Figure 1

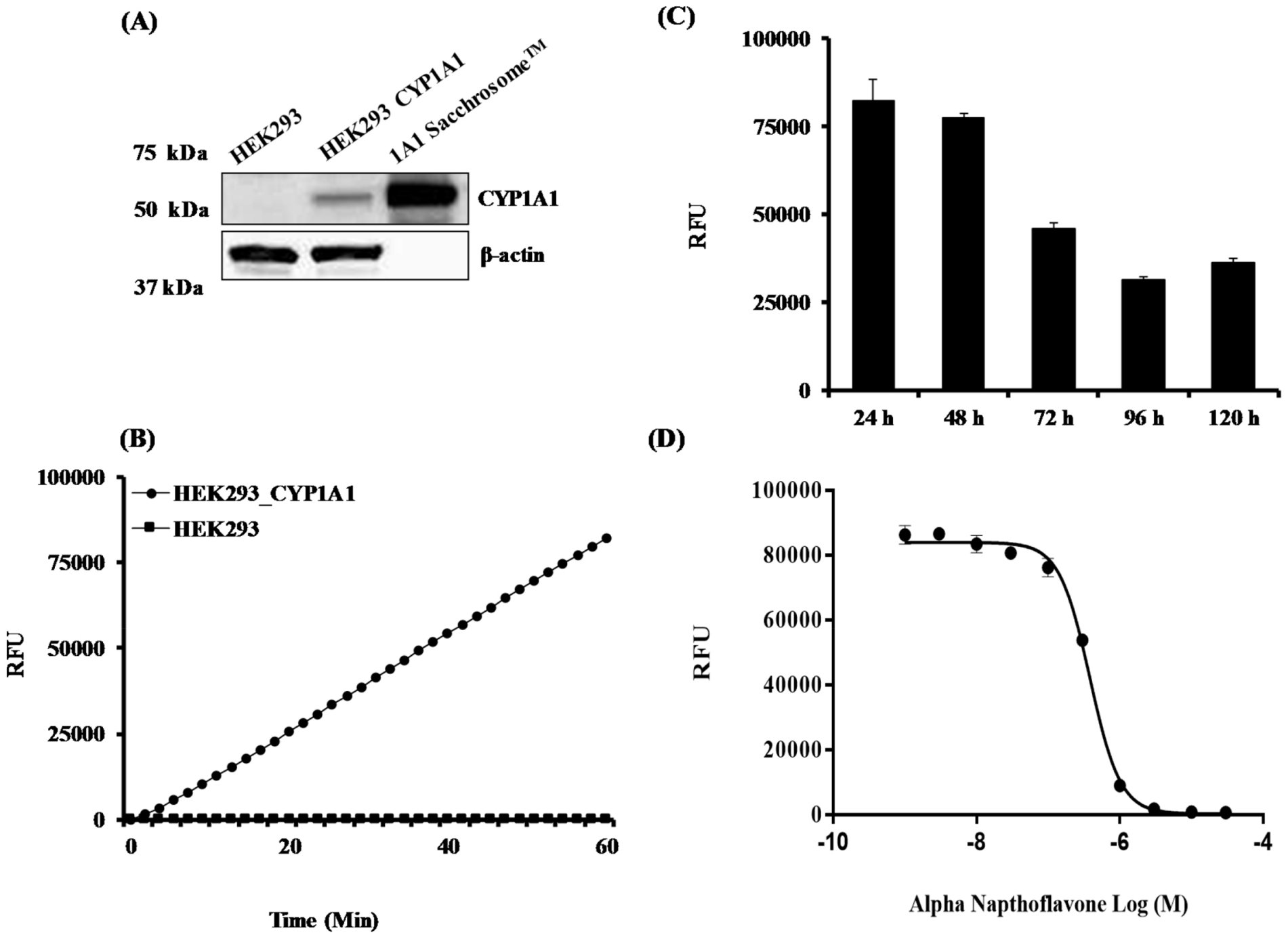
(A)
HEK293
HEK293 CYP1A1
1A1 Sacchrosome™
75 kDa
50 kDa
37 kDa
CYP1A1
β-actin
(B)
HEK293_CYP1A1
HEK293
RFU
Time (Min)
(C)
RFU
24 h
48 h
72 h
96 h
120 h
(D)
RFU
Alpha Napthoflavone Log (M)

Figure 2

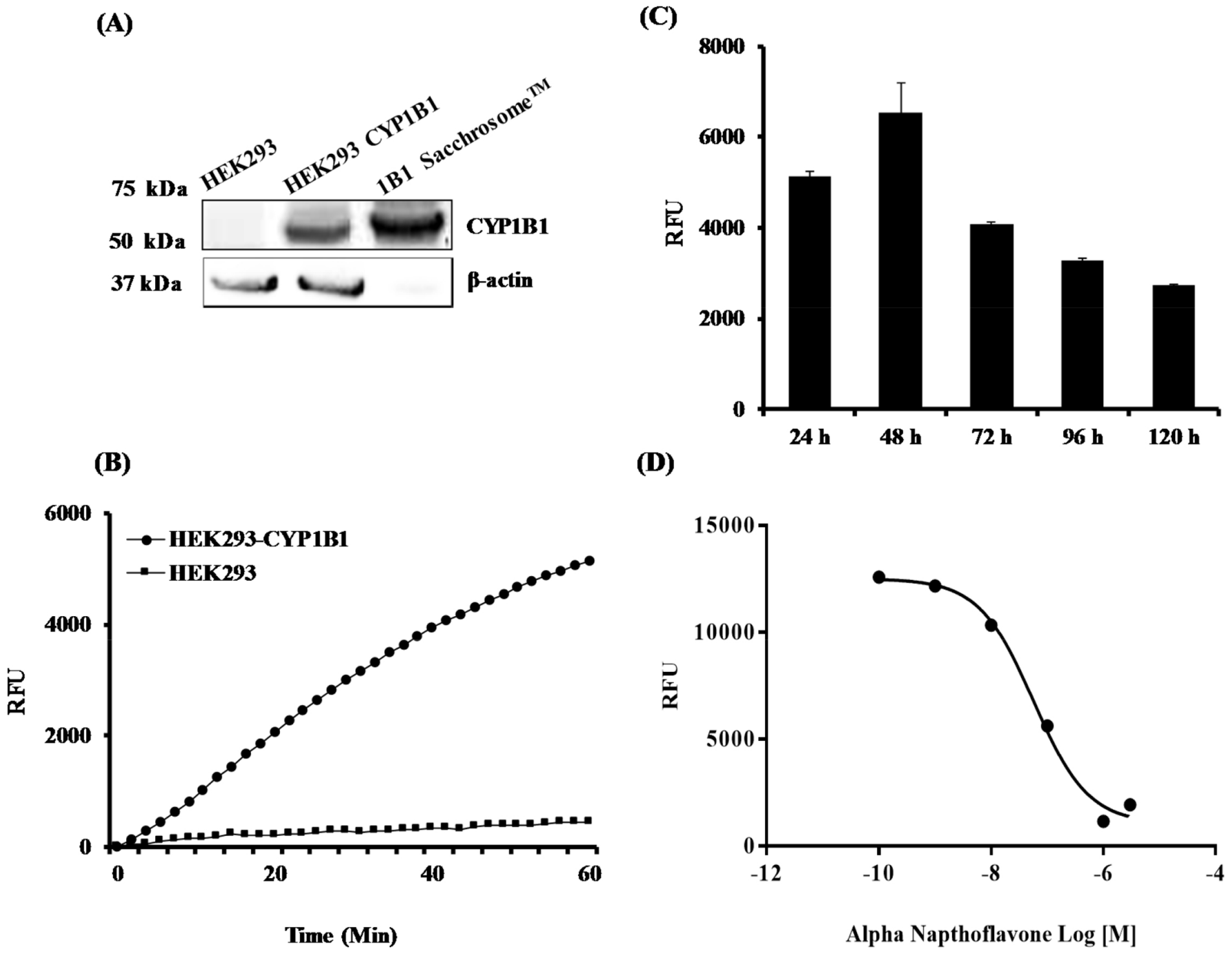
(A)
HEK293
HEK293 CYP1B1
1B1 Sacchrosome™
75 kDa
50 kDa
37 kDa
CYP1B1
β-actin
(C)
8000
6000
4000
2000
0
RFU
24 h
48 h
72 h
96 h
120 h
(B)
6000
4000
2000
0
RFU
HEK293-CYP1B1
HEK293
0
20
40
60
Time (Min)
(D)
15000
10000
5000
0
RFU
-12
-10
-8
-6
-4
Alpha Napthoflavone Log [M]

Figure 3

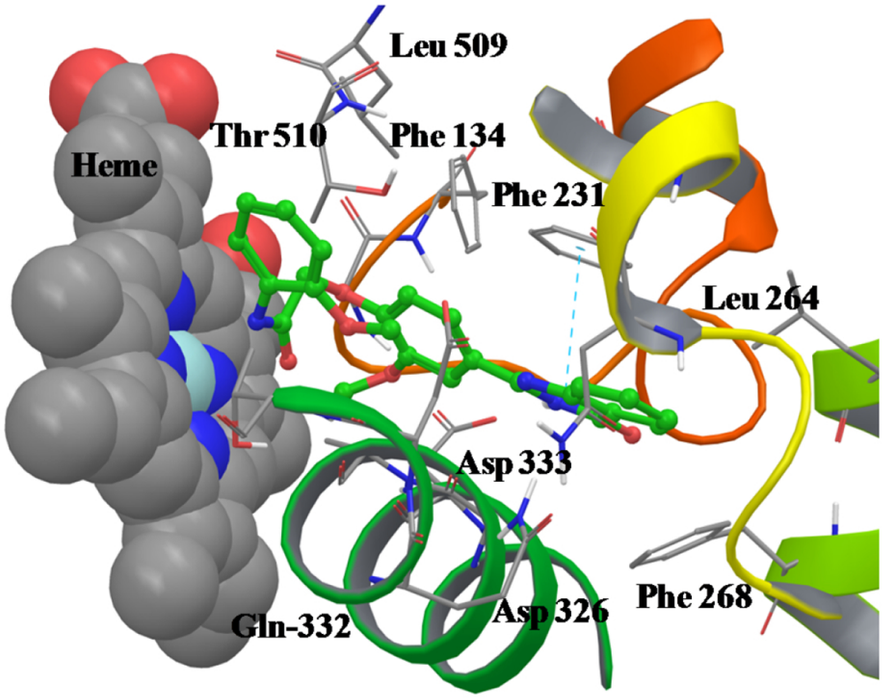
Leu 509
Thr 510
Phe 134
Heme
Phe 231
Leu 264
Asp 333
Phe 268
Asp 326
Gln-332

A.

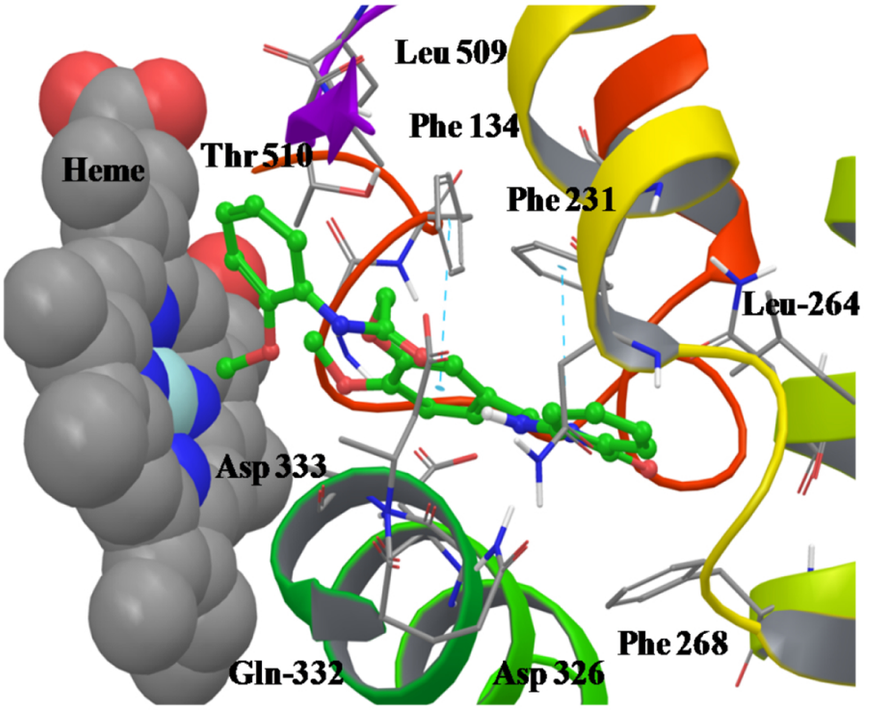
Leu 509
Phe 134
Thr 510
Heme
Phe 231
Leu-264
Asp 333
Phe 268
Gln-332
Asp 326

B.

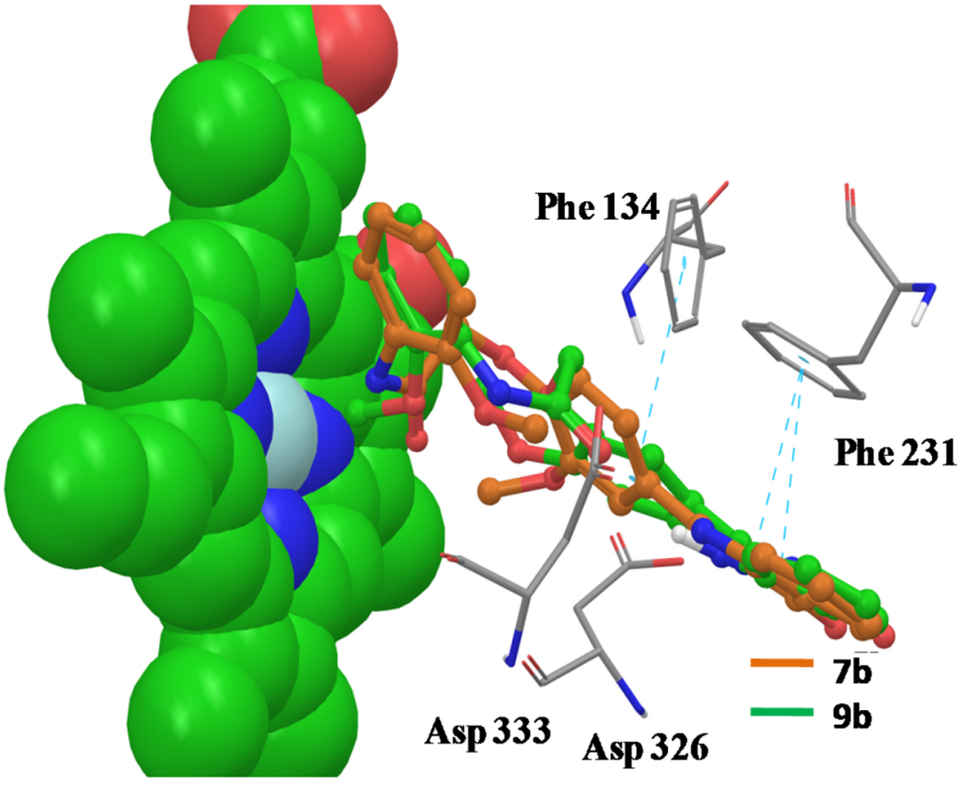
Phe 134
Phe 231
7b
9b
Asp 333
Asp 326

C.

Figure 4

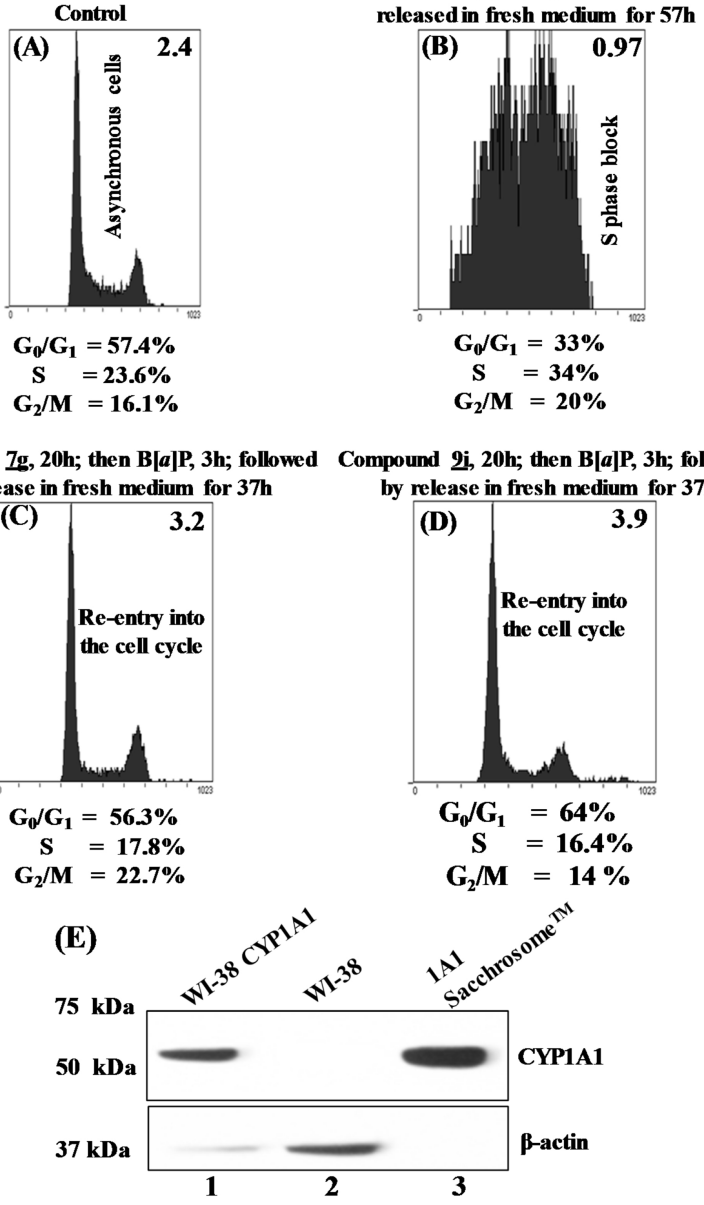
Control
(A)
2.4
Asynchronous cells
G_0/G_1 = 57.4%
S = 23.6%
G_2/M = 16.1%
B[a]P (3h), then released in fresh medium for 57h
(B)
0.97
S phase block
G_0/G_1 = 33%
S = 34%
G_2/M = 20%
Compound 7g, 20h; then B[a]P, 3h; followed by release in fresh medium for 37h
(C)
3.2
Re-entry into the cell cycle
G_0/G_1 = 56.3%
S = 17.8%
G_2/M = 22.7%
Compound 9i, 20h; then B[a]P, 3h; followed by release in fresh medium for 37h
(D)
3.9
Re-entry into the cell cycle
G_0/G_1 = 64%
S = 16.4%
G_2/M = 14 %
(E)
WI-38 CYP1A1
WI-38
1A1
Sacchrosome™
75 kDa
50 kDa
37 kDa
CYP1A1
β-actin
1
2
3

Figure 5

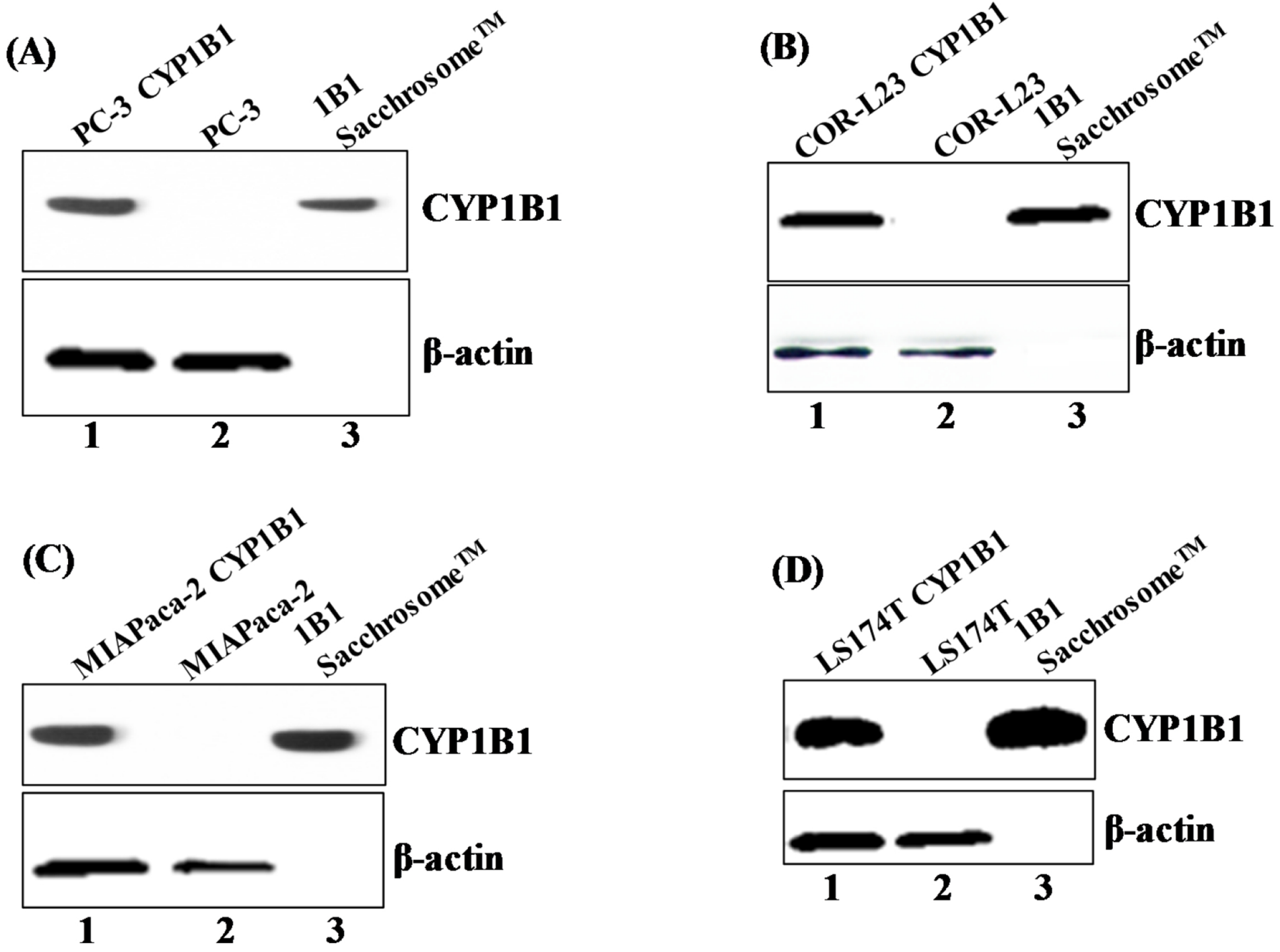
(A)
PC-3 CYP1B1
PC-3
1B1
Sacchrosome™
CYP1B1
β-actin
1
2
3
(B)
COR-L23 CYP1B1
COR-L23
1B1
Sacchrosome™
CYP1B1
β-actin
1
2
3
(C)
MIAPaca-2 CYP1B1
MIAPaca-2
1B1
Sacchrosome™
CYP1B1
β-actin
1
2
3
(D)
LS174T CYP1B1
LS174T
1B1
Sacchrosome™
CYP1B1
β-actin
1
2
3

Figure 6

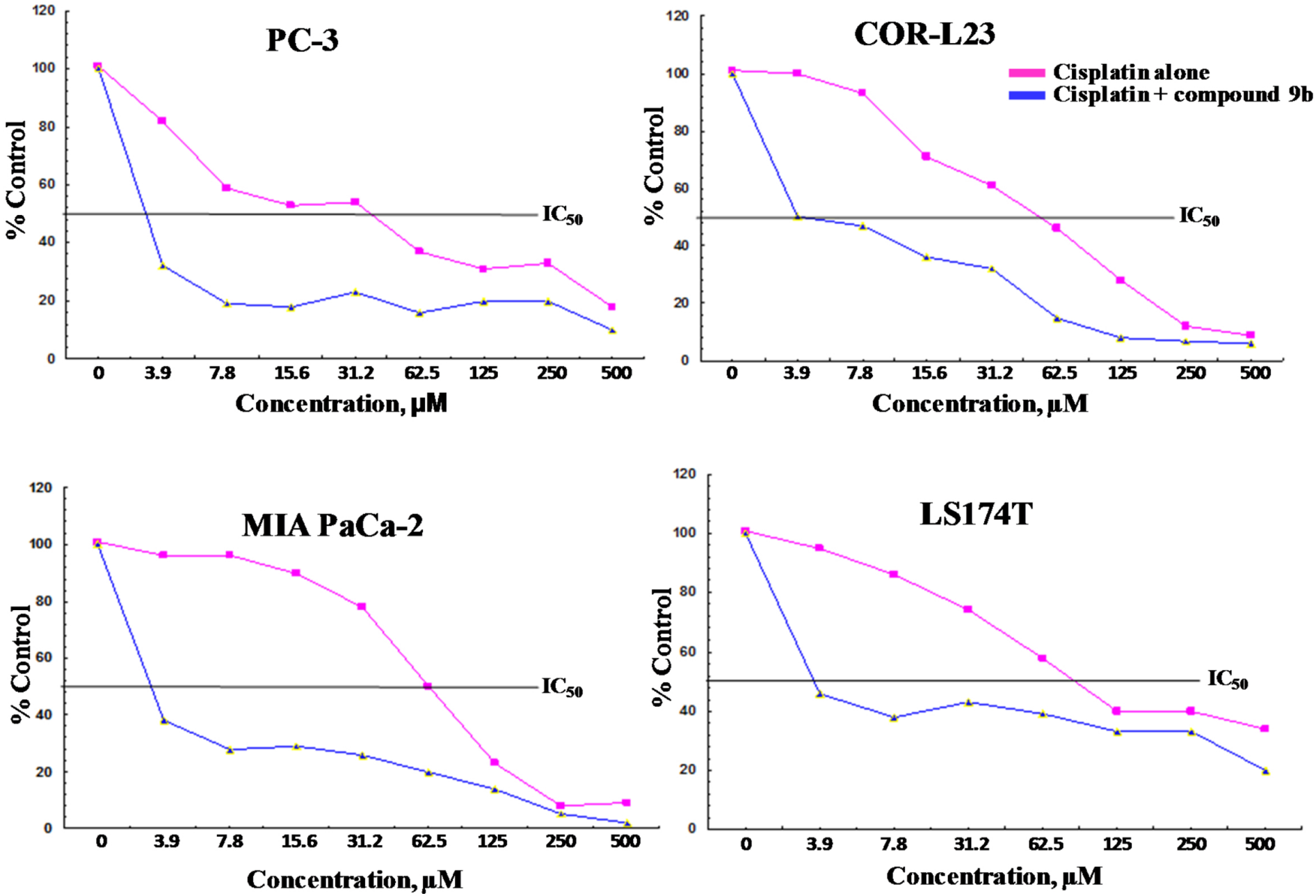
PC-3
COR-L23
MIA PaCa-2
LS174T
Cisplatin alone
Cisplatin + compound 9b
% Control
Concentration, µM
IC50
0
3.9
7.8
15.6
31.2
62.5
125
250
500
20
40
60
80
100
120

Figure 7

CP (3h), then released in fresh medium for 57h

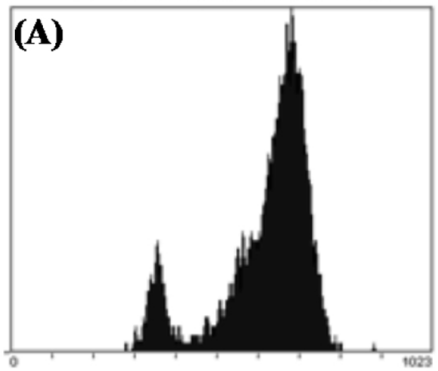

G_0/G_1 = 12%
S = 16%
G_2/M = 70%

G_2/M block

Cpd 5e (24h), CP (3h), then released in medium for 33h

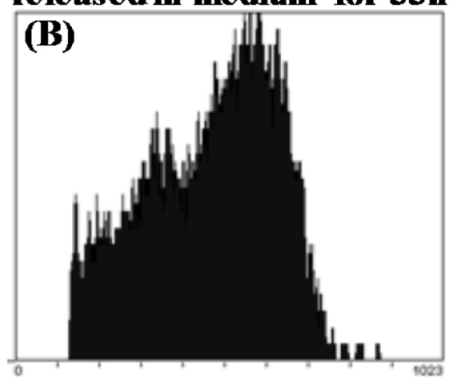

Sub-G_1 = 16.9%
G_0/G_1 = 19.6.%
S = 48%
G_2/M = 12%

S-phase block and apoptosis

Cpd 7b (24h), CP (3h), then released in medium for 33h

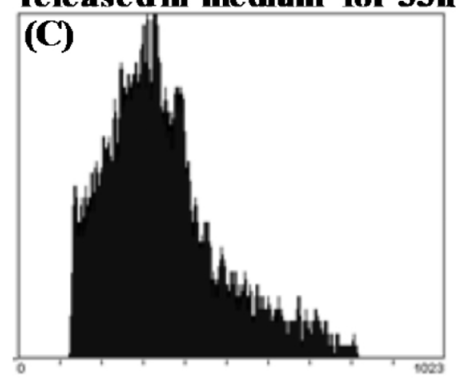

Sub-G_1 = 27%
G_0/G_1 = 34%
S = 31%
G_2/M = 5%

S-phase block and apoptosis

Cpd 7c (24h), CP (3h), then released in medium for 33h

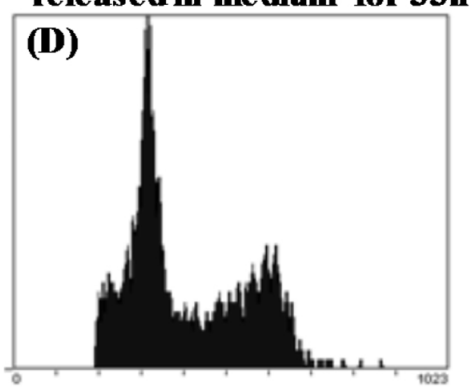

Sub-G_1 = 23%
G_0/G_1 = 32%
S = 25%
G_2/M = 13%

S-phase block and apoptosis

Cpd 9b (24h), CP (3h), then released in medium for 33h

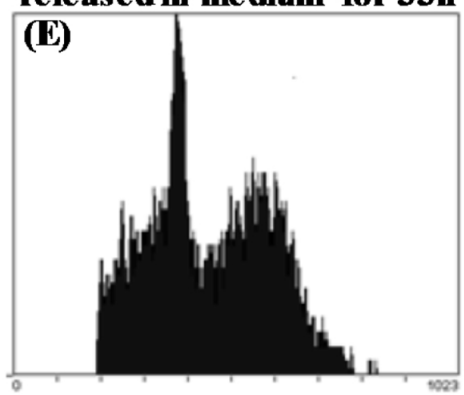

Sub-G_1 = 35%
G_0/G_1 = 17%
S = 36%
G_2/M = 10%

S-phase block and Apoptosis

Figure 8

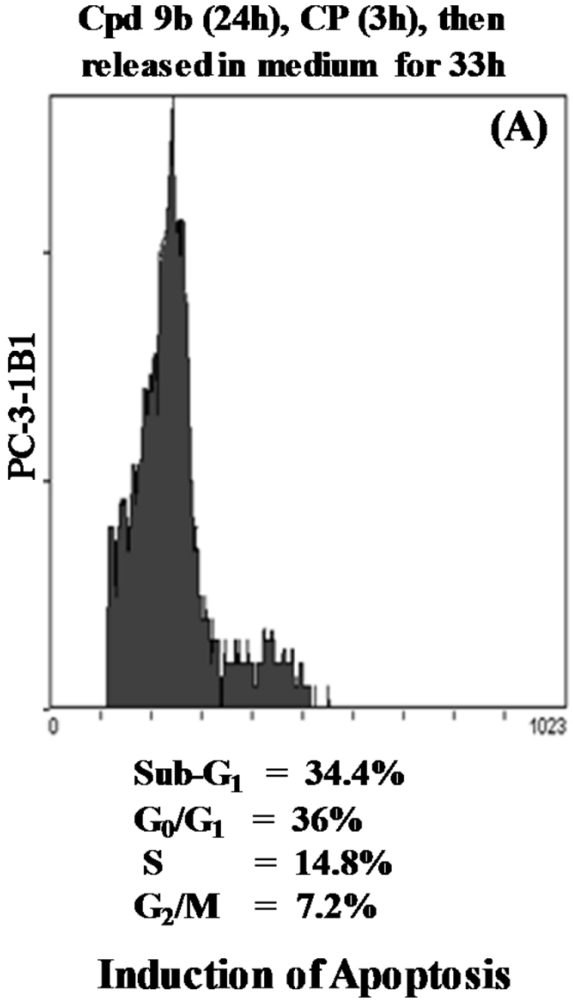
Cpd 9b (24h), CP (3h), then released in medium for 33h
(A)
PC-3-1B1
0
1023
Sub-G1 = 34.4%
G0/G1 = 36%
S = 14.8%
G2/M = 7.2%
Induction of Apoptosis

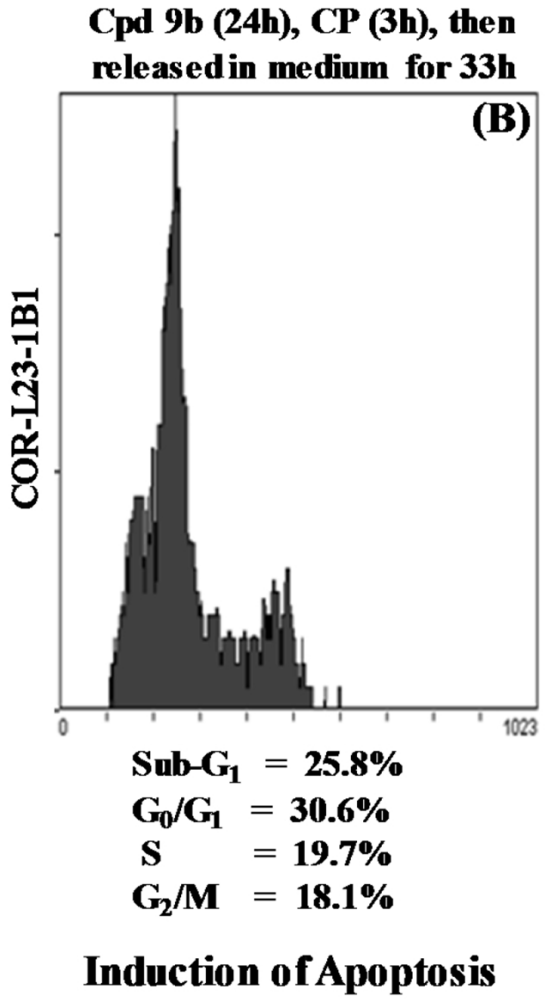
Cpd 9b (24h), CP (3h), then released in medium for 33h
(B)
COR-L23-1B1
0
1023
Sub-G1 = 25.8%
G0/G1 = 30.6%
S = 19.7%
G2/M = 18.1%
Induction of Apoptosis

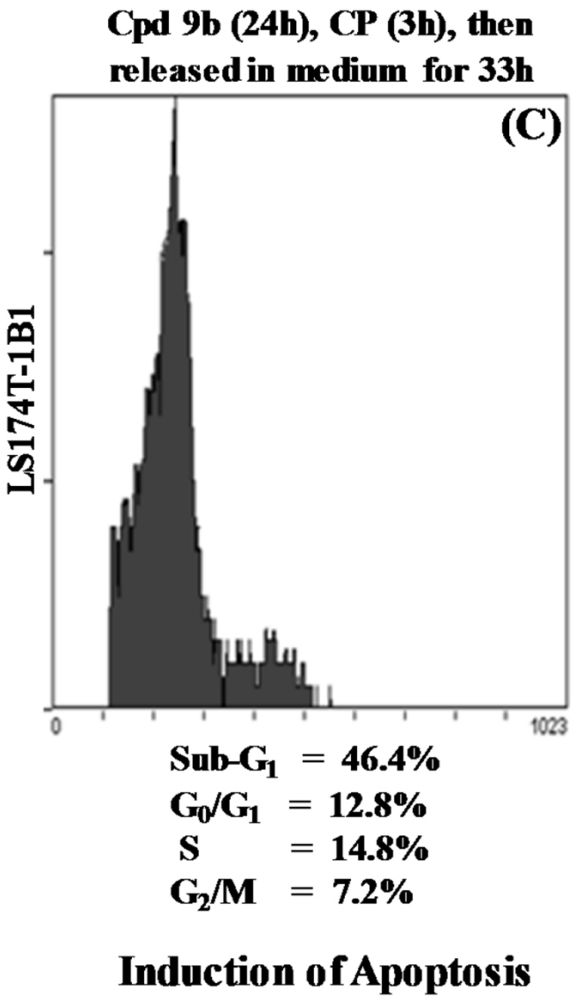
Cpd 9b (24h), CP (3h), then released in medium for 33h
(C)
LS174T-1B1
0
1023
Sub-G1 = 46.4%
G0/G1 = 12.8%
S = 14.8%
G2/M = 7.2%
Induction of Apoptosis

Figure 9